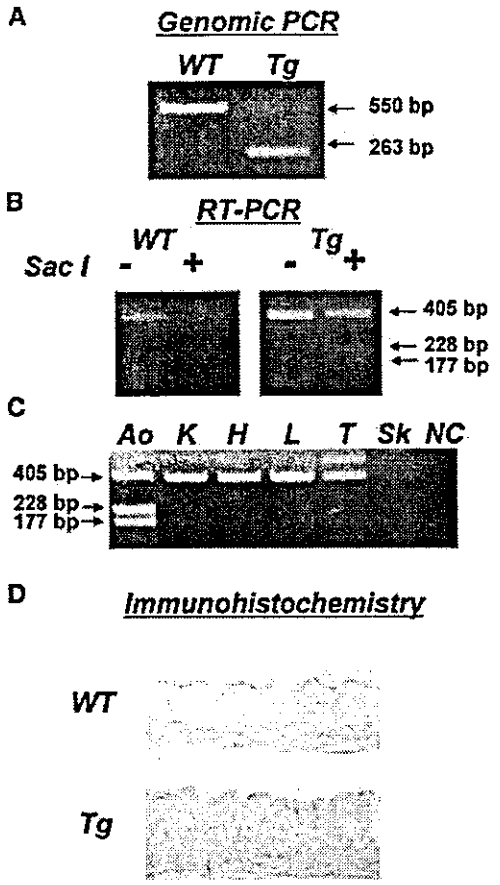

Figure 1. Characterization of mice with vascular smooth muscle–specific overexpression of biglycan. A, Representative result of PCR of tail DNA. Transgene yields a 263-bp PCR product, whereas the native biglycan gene yields a 550-bp PCR product. B, Representative result of *Sac*I digestion of RT-PCR product from aorta mRNA. RT-PCR product derived from the transgene mRNA yields 2 fragments (228 and 177 bp) after *Sac*I digestion. C, RT-PCR analysis of native and transgenic biglycan mRNA in aorta (Ao), kidney (K), heart (H), lung (L), testis (T), and skeletal muscle (Sk) of transgenic mice. All samples were digested with *Sac*I before electrophoresis to yield 2 fragments (228 and 177 bp) in the case of biglycan mRNA derived from the transgene, whereas the native biglycan mRNA is undigested (405 bp). NC indicates negative control. D, Immunohistochemical staining of wild-type (WT) and transgenic (Tg) mouse aorta using an anti-human biglycan antibody (LF-51).

immunohistochemical staining was performed. Positive staining for biglycan protein was substantially increased in the medial layer of biglycan-transgenic mice compared with their wild-type littermates (Figure 1D).

Effects of Biglycan Overexpression on the Aorta, Coronary Arteries, and Renal Arterioles

The effects of biglycan overexpression on the structure of large (aorta), medium-sized (coronary arteries), and small (renal arterioles) arteries were examined. Preliminary experiments suggested that proliferating cells in the vascular media stained by PCNA were increased compared with controls, resulting in increased medial thickness. To confirm these findings, mice were divided into 4 groups: groups 1 and 2 were wild-type mice, and groups 3 and 4 were transgenic mice. Groups 1 and 3 were treated with vehicle, whereas groups 2 and 4 were infused with a pressor dose of Ang II to accentuate vascular hypertrophy and hyperplasia. Online Table 1 (available in the online data supplement at http://circres.ahajournals.org) shows the results of changes in heart and body weight, blood pressure, and plasma renin activity in the groups with and without Ang II infusion. The initial body and heart weights were similar in the transgenic mice and wild-type mice, and the heart/body weight ratios were significantly increased after Ang II infusion in groups 2 and 4. Baseline systolic blood pressure did not differ significantly between the 4 groups. Ang II increased systolic blood pressure from 100±3 to 132±7 mm Hg in wild-type mice (group 2) and from 103±4 to 136±2 mm Hg in transgenic mice (group 4). We also measured PRA from blood samples of the 4 groups at the end of the study. PRA was below the detection level in the Ang II–treated groups (2 and 4). No significant change in PRA was found between the untreated wild-type and transgenic mice. The changes in native and transgenic biglycan mRNA in the Ang II–treated and –untreated groups are shown in Figure 2A. Consistent with our previous report,[4] Ang II treatment resulted in an increase in the native biglycan, but did not cause a significant change in the transgenic biglycan mRNA. Aortic and cardiac TGF-β1 mRNA was also increased by Ang II treatment, but no major differences were observed between wild-type and transgenic mice (Figures 2B and 2C).

Morphological changes in the aorta, coronary arteries, and renal arterioles were assessed. As shown in Figure 3, an increase in PCNA-positive cell counts was seen in the aorta of the transgenic mice compared with wild-type littermates. Moreover, increased media/lumen ratios were also seen in these vessels. Similar results were seen in the renal arterioles (Figure 4). In the case of the coronary arteries, more pronounced changes were seen (Figures 5 and 6). In the Masson-trichrome–stained sections, the effect of Ang II to cause cellular proliferation was accentuated in the biglycan transgenic mice, resulting in a dramatic proliferation of cells with areas of partial stenosis/occlusion of the coronary arteries in mice of group 4 (transgenic mice treated with Ang II) (Figure 5A). The incidence of coronary artery stenosis (defined as the presence of at least one lesion occupying >30% of the lumen) in the four groups of mice were as follows: wild-type Ang II (−) 0/15 (0%); wild-type Ang II (+) 2/15 (13%); transgenic Ang II (−) 0/18 (0%); and transgenic Ang II (+) 16/26 (62%).

The prominent lesions seen in the transgenic mice treated with Ang II were examined immunohistochemically. Quantitation of PCNA-positive cell counts revealed significant elevation in the transgenic mice with or without Ang II infusion compared with wild-type mice (Figure 5B). To characterize the cell types responsible for the stenotic lesions, staining was also performed using specific markers. It was found that the intimal cells stained strongly for α-smooth muscle cell actin, suggesting that the cells were derived from proliferating vascular smooth muscle cells (Figure 6).

We also assessed perivascular fibrosis in the coronary arteries by measurement of the fibrotic index. Both untreated

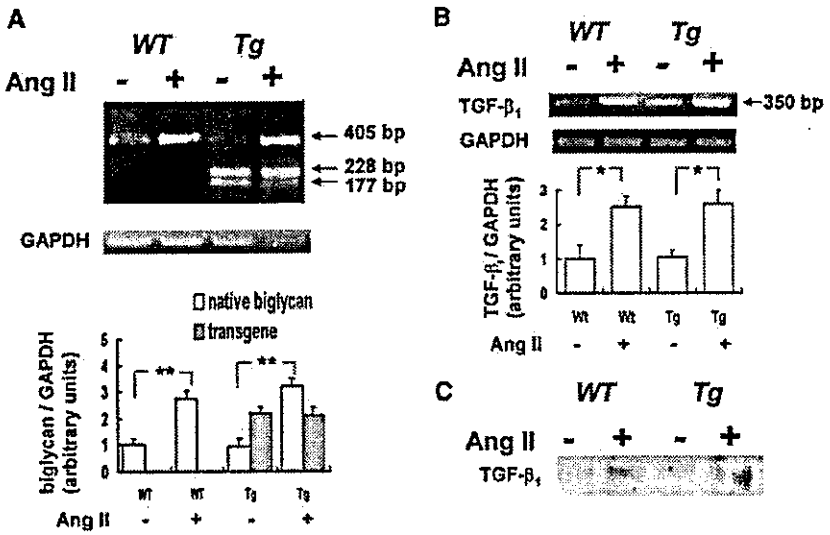

Figure 2. A, RT-PCR-RFLP analysis of biglycan mRNA from the aorta of wild-type (WT) and transgenic (Tg) mice with and without Ang II treatment. All samples were digested with *SacI* before electrophoresis to yield 2 fragments (228 and 177 bp) in the case of biglycan mRNA derived from the transgene, whereas the native biglycan mRNA is undigested (405 bp). Top, Representative result of RT-PCR analysis. Bottom, Results of densitometric analysis; $^{**}P<0.01$ (n=5 per group). B, RT-PCR analysis of TGF-β_1 mRNA from the aorta of wild-type (WT) and transgenic (Tg) mice with and without Ang II treatment; $^{*}P<0.05$ (n=5 per group). C, Western blot analysis of TGF-β_1 in the hearts of wild-type (WT) and transgenic (Tg) mice with and without Ang II treatment.

and Ang II–treated transgenic mice showed increased fibrotic index compared with the wild-type mice (Figure 5C). Assessment of cardiac collagen content was also performed by measuring hydroxyproline content in cardiac sections. Although baseline cardiac collagen content did not differ significantly between the transgenic and the wild-type mice, Ang II treatment resulted in a greater increase (1.7-fold change from 1.13±0.14 to 1.90±0.20 μmol/g; $P<0.05$) in the transgenic mice compared with wild-type mice (1.2-fold change from 1.30±0.29 to 1.55±0.28 μmol/g; P=NS).

Effects of Biglycan on VSMC Proliferation, Collagen Synthesis, and Migration In Vitro

To further examine the effects of biglycan on the vasculature, experiments were performed on cultured vascular cells (VSMCs and endothelial cells) in vitro. Figure 7 shows the effects of biglycan on VSMC growth. Biglycan caused an increase in VSMC numbers, and a dose-dependent increase in thymidine incorporation by VSMCs, whereas an opposite trend was found in thymidine incorporation in the case of endothelial cells. The effects of biglycan were additive with the effects of Ang II. Biglycan also caused a significant increase in collagenase-sensitive proline incorporation in Ang II–treated VSMCs but not in endothelial cells.

We next examined the migratory response to biglycan in VSMC and endothelial cells. As shown in Figure 7, biglycan treatment elicited a robust migratory response in VSMCs, and further enhanced the Ang II–induced migratory response. In contrast, no apparent change was seen in endothelial cell migration.

Western Blot Analysis of Intracellular Signaling Pathways of Biglycan in Vascular Cells

The effects of biglycan on the expression of genes affecting VSMC proliferation were examined by Western blot analysis. As shown in Figure 8, stimulation with biglycan resulted in an enhancement of cdk2 expression within 6 hours in VSMCs. In contrast, levels of p27 were reduced at 24 hours, whereas p21 expression remained at low levels throughout the experiment.

Discussion

Biglycan is a major glycoprotein of the extracellular matrix.[1–3] Biochemically, it belongs to the SLRP family of proteoglycans and is composed of a distinct core protein covalently bound to two chondroitin sulfate/dermatan sulfate-containing glycosaminoglycan side chains.

The functions of biglycan are only beginning to be understood. Similar to decorin, biglycan has been shown to bind TGF-β in vitro[16]; however, there is controversy whether biglycan exerts TGF-β inhibitory effects in vivo.[17] Biglycan has also been shown to associate with type I[18] and type VI[19] collagens in vitro, suggesting a role in the control of collagen fibrillogenesis. Indeed, targeted disruption of the biglycan gene results in a phenotype characterized by abnormal collagen fibrils in tendons, together with abnormal bone structure and reduced bone mass.[20,21]

Biglycan is known to be expressed in the arterial wall and has been purified from the normal human aorta.[22] However, the role of biglycan in the vasculature is unclear. Of note is the fact that expression of biglycan is markedly upregulated in diseased arteries, including atherosclerotic lesions,[9] arteriolosclerotic lesions,[23] areas of restenosis postangioplasty,[10] and in transplant coronary arteriopathy.[24] Of interest, it has been reported that biglycan colocalizes with apolipoprotein E in atherosclerotic plaques,[9] suggesting the hypothesis that biglycan, by virtue of its ability to bind apolipoproteins, may be directly involved in the retention of these atherogenic molecules in the diseased vessel wall.

Because the upregulation of biglycan in diseased arteries suggested a role in vascular disease, our aim in this study was to examine the direct consequences of increasing biglycan content in the vessel wall. To this end, transgenic mice that overexpressed biglycan in the vasculature were produced using a transgene construct consisting of the human biglycan cDNA ligated downstream of the smooth muscle cell α-actin promoter. Experiments were performed on two transgenic lines that yielded similar results.

No gross changes in the development or behavior of the transgenic mice were observed compared with their nontrans-

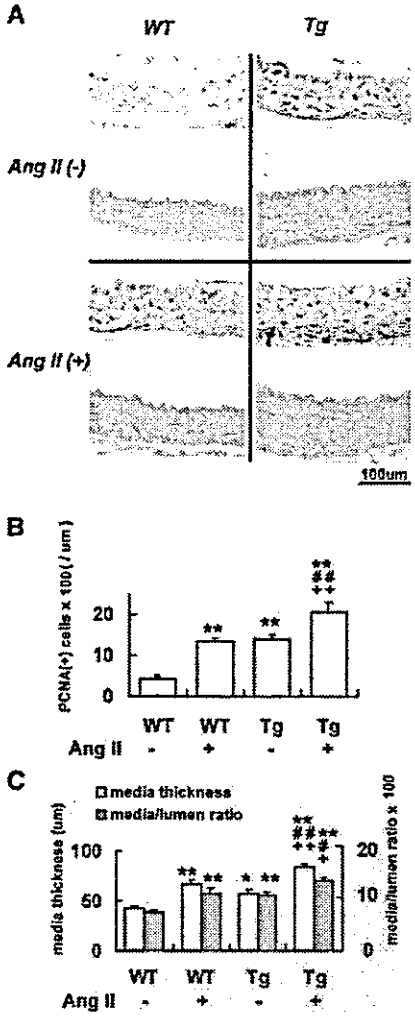

Figure 3. Vascular morphology of aorta of wild-type (WT) and transgenic (Tg) mice with and without Ang II treatment. A, Representative cross sections of aortic wall. Top photomicrograph, PCNA immunostaining; bottom photomicrograph, Azan stain. Original magnification ×100. B, Quantitation of PCNA-positive cell counts in aorta of wild-type and transgenic mice. C, Quantitation of media thickness and media/lumen ratios in aorta of wild-type and transgenic mice.*P<0.05, **P<0.01 vs wild-type [Ang II (−)]; +P<0.05, ++P<0.01 vs Tg [Ang II (−)]: #P<0.05, ##P<0.01 vs wild-type [Ang II (+)] (n=8 to 16 per group).

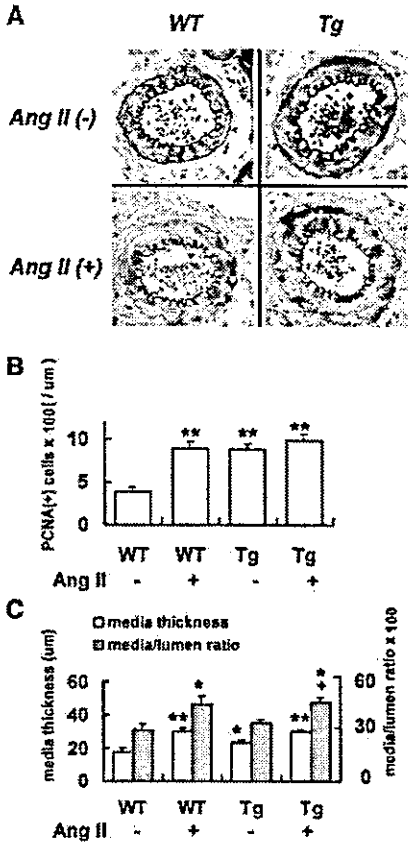

Figure 4. Vascular morphology of renal arterioles of wild-type (WT) and transgenic (Tg) mice with and without Ang II treatment. A, Representative Azan stain of renal arteriole wall. B, Quantitation of PCNA-positive cell counts in renal arterioles of wild-type and transgenic mice. C, Quantitation of media thickness and media/lumen ratios in renal arteriole of wild-type and transgenic mice. *P<0.05, **P<0.01 vs wild-type [Ang II (−)]; +P<0.05 vs Tg [Ang II (−)] (n=8 to 16 per group).

genic littermates. Moreover cardiac echocardiography did not reveal a major difference in ejection fraction between untreated transgenic and wild-type mice (data not shown). However, increased proliferation of the aortic wall and renal arterioles was seen, which was evidenced by increased numbers of PCNA-positive cells in these vessels, accompanied by increases in the medial thickness of the vessels.

In this study, we examined the effects of infusion of Ang II on the vasculature in wild-type and transgenic mice, because Ang II is a peptide hormone that is thought to play a major role in the progression of vascular disease, a concept which has been underscored by the efficacy of Ang receptor blockade in attenuating the progression of hypertensive vascular disease. Ang II infusion resulted in an increase in vascular hypertrophy and proliferation of vascular cells, and these effects were enhanced in the aorta of the transgenic the mice. Another notable finding were the lesions seen in the coronary arteries of the Ang II–infused transgenic mice, which were reminiscent of vascular lesions in coronary disease, with marked increases in the vascular intima, resulting in some cases in partial occlusion of coronary arteries, together with increases in perivascular fibrosis.

Concerning the mechanisms of these changes, we found that stimulation of VSMCs with biglycan resulted in an increase in thymidine incorporation, an effect that was additive with Ang II. These results were consistent with the in vivo findings in the transgenic mice and provided further evidence that biglycan has a proliferative effect on VSMCs.

It is well known that VSMC proliferation is coordinately regulated by cell cycle proteins. Activation of a cdk2-cyclin complex during the G1 phase is involved in the G1 to S phase transition, and this complex is inhibited by the cdk inhibitor p27.[25] Therefore, our findings that biglycan enhances cdk2 kinase expression while diminishing p27 levels is consistent with the proliferative effects of biglycan that we found both in vivo and in vitro. It has been suggested that cell cycle

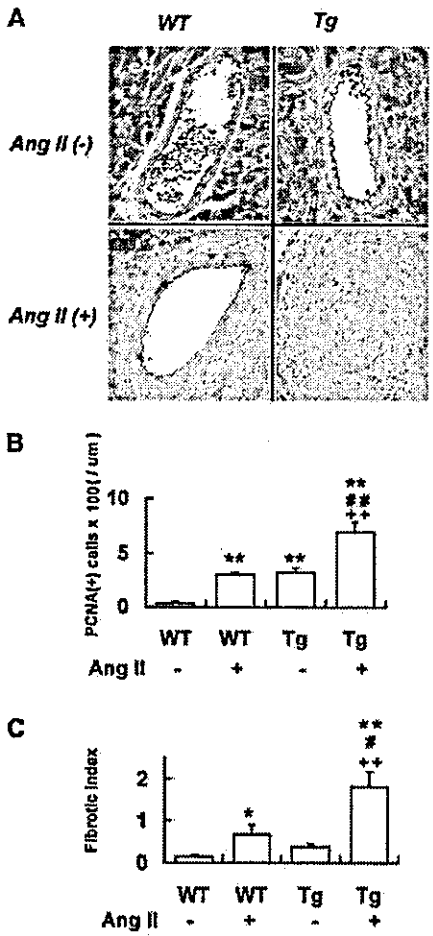

Figure 5. Vascular and perivascular morphology of coronary arteries of wild-type (WT) and transgenic (Tg) mice with and without Ang II treatment. A, Representative micrographs of coronary artery sections stained with Masson-trichrome in wild-type and transgenic mice. Original magnification ×200. B, Quantitation of PCNA-positive cell counts in coronary arteries of wild-type and transgenic mice. C, Quantitation of perivascular fibrosis in coronary arteries of wild-type and transgenic mice. *$P<0.05$, **$P<0.01$ vs wild-type [Ang II (−)]; ++$P<0.01$ vs Tg [Ang II (−)]: #$P<0.05$, ##$P<0.01$ vs Wild-type [Ang II (+)] (n=8 to 16 per group).

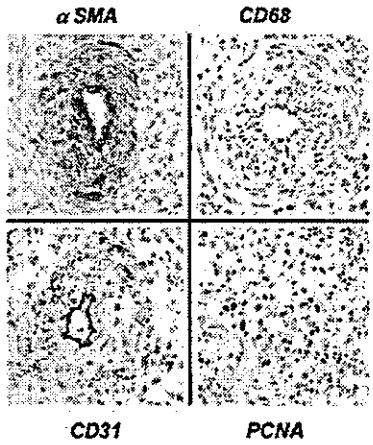

Figure 6. Immunohistochemical assessment of coronary lesions in Ang II–treated transgenic mice. A, Results of immunostaining of coronary arteries from Ang II–infused transgenic mice with antibodies to α-smooth muscle cell actin (αSMA), CD68 (marker for macrophages), CD31 (marker for endothelial cells), and PCNA. Original magnification ×200.

proteins may also regulate VSMC migration.[26] Taken together, our results suggest that the observed phenotype in the biglycan transgenic mice could be explained by the effects on these intracellular proteins.

It should be noted that the proliferative effects of biglycan appeared to depend on the cell type, because biglycan caused a decrease in thymidine incorporation in cultured endothelial cells in clear contrast to the effects on VSMCs. Similarly, biglycan increased migration in VSMCs but not in endothelial cells. With regards to the effects of biglycan on other cells, biglycan has been suggested to stimulate growth and differentiation of monocytic lineage cells and brain microglial cells, whereas in pancreatic cancer cells proliferation was suppressed by biglycan, and in mesangial cells biglycan had no significant effect alone, but inhibited the proliferative effects of PDGF-BB.[27–29] Of further interest is the fact that the related SLRP decorin has been shown to induce p21, p27, and growth arrest in many cell types including both VSMCs and endothelial cells.[30,31] Taken together, these results suggest that biglycan and decorin found in the extracellular matrix may be involved in the cell-specific regulation of cell proliferation and growth. It remains to be determined whether the differences between biglycan and decorin exist because of differences in the core protein structure, or the number of glycosaminoglycan side-chains associated with these two related molecules.

In the in vivo experiments using biglycan transgenic mice, we did not differentiate between the influence of Ang II per se on the vasculature, versus the indirect effects of the increased blood pressure mediated by Ang II. Because comparable results were seen in cultured VSMCs in vitro, it is probable that the effects on cell growth and perivascular fibrosis in vivo may be attributed at least in part to biglycan modulating a direct (blood pressure–independent) effect of Ang II on the vasculature in the transgenic mice. However, the possibility that a blood pressure–mediated mechanism could also contribute to the changes cannot be ruled out. Another possibility is that changes in growth factor expression could be involved as an intermediary mechanism. The fact that major differences in TGF-β1 mRNA were not found between the wild-type and transgenic mice suggest that changes in the expression of this growth factor do not play a major role in the observed changes.

The results of this study have several implications for the understanding of vascular biology and the pathogenesis of vascular injury. In designing the study, our initial hypothesis was that biglycan overexpression would result in an attenuation of vascular injury, because the related SLRP decorin is a potential candidate for the gene therapy of diseases such as postangioplasty restenosis, pulmonary fibrosis, and renal glomerulosclerosis.[32–34] In fact, the results of this study suggest that the upregulation of biglycan reported in diseased arteries may contribute directly to the pathogenesis of vascu-

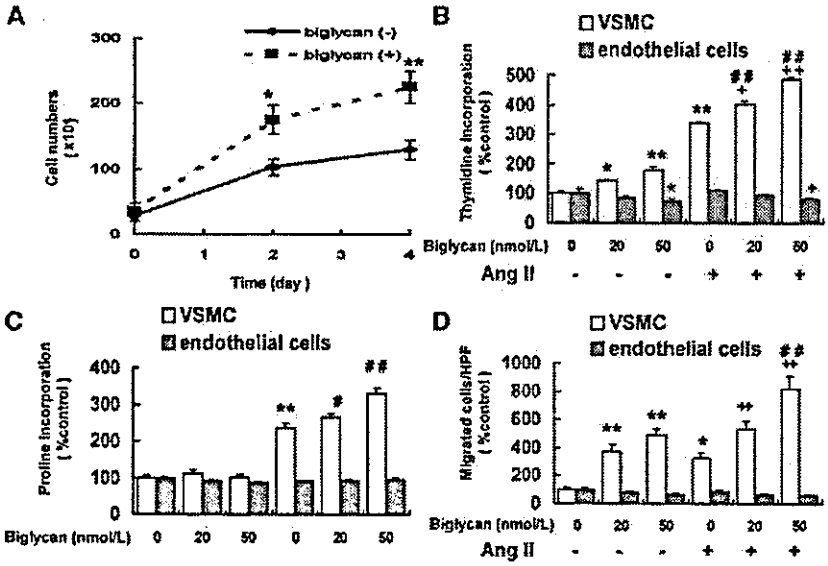

Figure 7. Effects of biglycan and Ang II on cell numbers (A), thymidine incorporation (B), collagen synthesis (C), and cell migration (D) in VSMCs and endothelial cells. *P<0.05, **P<0.01 vs biglycan (−), Ang II (−); +P<0.05, ++P<0.01 vs biglycan (−), Ang II (+): #P<0.05, ##P<0.01 vs corresponding values for biglycan (+), Ang II (−) (n=4).

lar disease, instead of being solely a secondary response to vascular injury. It is well known that susceptibility to vascular stenosis or atherosclerosis differs markedly between individuals and between different arteries within the same individual. The hypothesis that differences in biglycan expression may account for some of these differences requires investigation. Similarly, our observation that the effects of biglycan on cell growth depends on the cell type may be useful not only for understanding the mechanisms of growth regulation of vascular cells in the presence of different types of extracellular matrix, but also may be of future benefit for designing strategies for accelerating the proliferation of one type of cell over another.

In summary, we have shown that overexpression of the extracellular matrix proteoglycan biglycan in the blood vessel to levels similar to those found in diseased arteries results in an increase in vascular hypertrophy, proliferation, and a heightened susceptibility of the coronary arteries to Ang

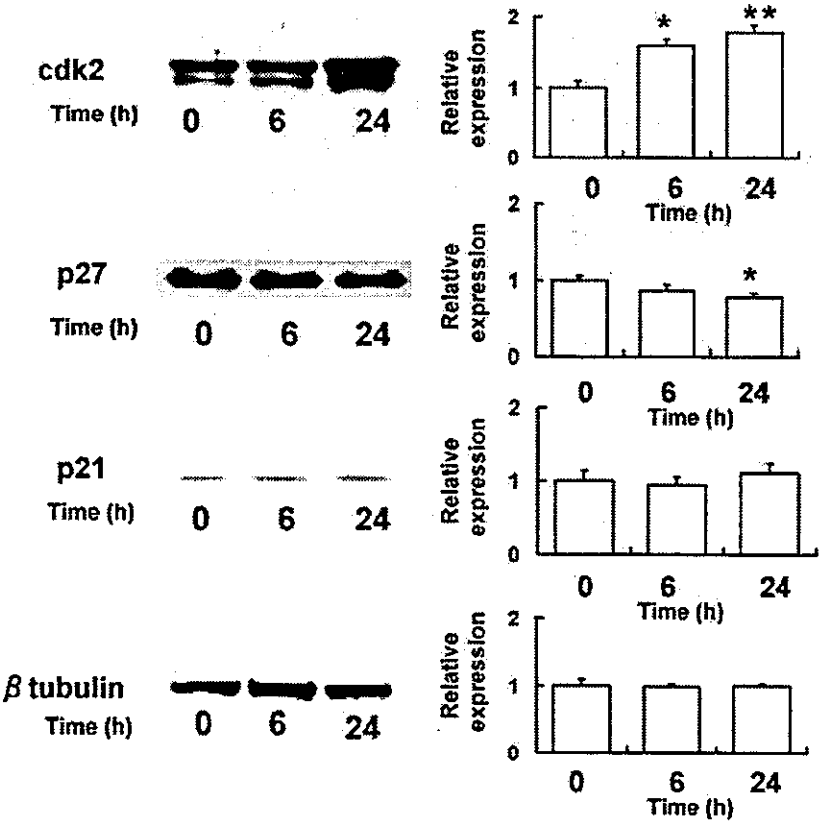

Figure 8. Effect of biglycan (50 nmol/L) on cdk2 kinase (A), p27 (B), p21 (C), and β-tubulin (D) levels in VSMCs. Left, Representative Western blot. Right, Results of densitometric analysis. Densitometric data were normalized to β-tubulin and expressed as relative levels compared with control (0 hour). *P<0.05, **P<0.01 vs control (n=4).

II–induced vascular injury and perivascular fibrosis. These effects may be mediated at least in part by changes in cell cycle–regulatory proteins. These results reinforce the concept that molecules in the extracellular matrix can affect the behavior of the surrounding smooth muscle cells and may have important implications for our understanding of the processes influencing vascular injury.

Acknowledgments

This study was supported by grants from the Ministry of Science and Education, Japan. The authors are grateful to Dr Tomomi Meguro in the laboratory of Dr Tsutomu Yoshikawa, Division of Cardiology, Department of Internal Medicine, School of Medicine, Keio University, for echocardiographic examination of the transgenic mice and to Dr Tatsuo Shimosawa, Department of Nephrology, University of Tokyo, for helpful comments and advice.

References

1. Iozzo RV. Matrix proteoglycans: from molecular design to cellular function. *Annu Rev Biochem.* 1998;67:609–652.
2. Fisher LW, Termine JD, Young MF. Deduced protein sequence of bone small proteoglycan I (biglycan) shows homology with proteoglycan II (decorin) and several nonconnective tissue proteins in a variety of species. *J Biol Chem.* 1989;264:4571–4576.
3. Hocking AM, Shinomura T, McQuillan DJ. Leucine-rich repeat glycoproteins of the extracellular matrix. *Matrix Biol.* 1998;17:1–19.
4. Shimizu-Hirota R, Sasamura H, Mifune M, Nakaya H, Kuroda M, Hayashi M, Saruta T. Regulation of vascular proteoglycan synthesis by angiotensin II type 1 and type 2 receptors. *J Am Soc Nephrol.* 2001;12:2609–2615.
5. Sasamura H, Shimizu-Hirota R, Nakaya H, Saruta T. Effects of AT1 receptor antagonist on proteoglycan gene expression in hypertensive rats. *Hypertens Res.* 2001;24:165–172.
6. Kuroda M, Sasamura H, Shimizu-Hirota R, Mifune M, Nakaya H, Kobayashi E, Hayashi M, Saruta T. Glucocorticoid regulation of proteoglycan synthesis in mesangial cells. *Kidney Int.* 2002;62:780–789.
7. Kunjathoor VV, Chiu DS, O'Brien KD, LeBoeuf RC. Accumulation of biglycan and perlecan, but not versican, in lesions of murine models of atherosclerosis. *Arterioscler Thromb Vasc Biol.* 2002;22:462–468.
8. Yamakawa T, Bai HZ, Masuda J, Sawa Y, Shirakura R, Ogata J, Matsuda H. Differential expression of proteoglycans biglycan and decorin during neointima formation after stent implantation in normal and atherosclerotic rabbit aortas. *Atherosclerosis.* 2000;152:287–297.
9. O'Brien KD, Olin KL, Alpers CE, Chiu W, Ferguson M, Hudkins K, Wight TN, Chait A. Comparison of apolipoprotein and proteoglycan deposits in human coronary atherosclerotic plaques: colocalization of biglycan with apolipoproteins. *Circulation.* 1998;98:519–527.
10. Riessen R, Isner JM, Blessing E, Loushin C, Nikol S, Wight TN. Regional differences in the distribution of the proteoglycans biglycan and decorin in the extracellular matrix of atherosclerotic and restenotic human coronary arteries. *Am J Pathol.* 1994;144:962–974.
11. Nakano Y, Nishihara T, Sasayama S, Miwa T, Kamada S, Kakunaga T. Transcriptional regulatory elements in the 5′ upstream and first intron regions of the human smooth muscle (aortic type) α-actin-encoding gene. *Gene.* 1991;99:285–289.
12. Li J, Schwimmbeck PL, Tschope C, Leschka S, Husmann L, Rutschow S, Reichenbach F, Noutsias M, Kobalz U, Poller W, Spillmann F, Zeichhardt H, Schultheiss HP, Pauschinger M. Collagen degradation in a murine myocarditis model: relevance of matrix metalloproteinase in association with inflammatory induction. *Cardiovasc Res.* 2002;56:235–247.
13. Susic D, Francischetti A, Frohlich ED. Prolonged L-arginine on cardiovascular mass and myocardial hemodynamics and collagen in aged spontaneously hypertensive rats and normal rats. *Hypertension.* 1999;33:451–455.
14. Mifune M, Sasamura H, Shimizu-Hirota R, Miyazaki H, Saruta T. Angiotensin II type 2 receptors stimulate collagen synthesis in cultured vascular smooth muscle cells. *Hypertension.* 2000;36:845–850.
15. Nozawa Y, Matsuura N, Miyake H, Yamada S, Kimura R. Effects of TH-142177 on angiotensin II-induced proliferation, migration and intracellular signaling in vascular smooth muscle cells and on neointimal thickening after balloon injury. *Life Sci.* 1999;64:2061–2070.
16. Hildebrand A, Romaris M, Rasmussen LM, Heinegard D, Twardzik DR, Border WA, Ruoslahti E. Interaction of the small interstitial proteoglycans biglycan, decorin and fibromodulin with transforming growth factor β. *Biochem J.* 1994;302(pt 2):527–534.
17. Kolb M, Margetts PJ, Sime PJ, Gauldie J. Proteoglycans decorin and biglycan differentially modulate TGF-β-mediated fibrotic responses in the lung. *Am J Physiol Lung Cell Mol Physiol.* 2001;280:L1327–L1334.
18. Schonherr E, Witsch-Prehm P, Harrach B, Robenek H, Rauterberg J, Kresse H. Interaction of biglycan with type I collagen. *J Biol Chem.* 1995;270:2776–2783.
19. Wiberg C, Heinegard D, Wenglen C, Timpl R, Morgelin M. Biglycan organizes collagen VI into hexagonal-like networks resembling tissue structures. *J Biol Chem.* 2002;277:49120–49126.
20. Ameye L, Aria D, Jepsen K, Oldberg A, Xu T, Young MF. Abnormal collagen fibrils in tendons of biglycan/fibromodulin-deficient mice lead to gait impairment, ectopic ossification, and osteoarthritis. *FASEB J.* 2002;16:673–680.
21. Xu T, Bianco P, Fisher LW, Longenecker G, Smith E, Goldstein S, Bonadio J, Boskey A, Heegaard AM, Sommer B, Satomura K, Dominguez P, Zhao C, Kulkarni AB, Robey PG, Young MF. Targeted disruption of the biglycan gene leads to an osteoporosis-like phenotype in mice. *Nat Genet.* 1998;20:78–82.
22. Shirk RA, Parthasarathy N, San Antonio JD, Church FC, Wagner WD. Altered dermatan sulfate structure and reduced heparin cofactor II-stimulating activity of biglycan and decorin from human atherosclerotic plaque. *J Biol Chem.* 2000;275:18085–18092.
23. Stokes MB, Holler S, Cui Y, Hudkins KL, Eitner F, Fogo A, Alpers CE. Expression of decorin, biglycan, and collagen type I in human renal fibrosing disease. *Kidney Int.* 2000;57:487–498.
24. Lin H, Wilson JE, Roberts CR, Horley KJ, Winters GL, Costanzo MR, McManus BM. Biglycan, decorin, and versican protein expression patterns in coronary arteriopathy of human cardiac allograft: distinctness as compared to native atherosclerosis. *J Heart Lung Transplant.* 1996;15:1233–1247.
25. Hengst L, Reed SI. Translational control of p27Kip1 accumulation during the cell cycle. *Science.* 1996;271:1861–1864.
26. Boehm M, Nabel EG. Cell cycle and cell migration: new pieces to the puzzle. *Circulation.* 2001;103:2879–2881.
27. Weber CK, Sommer G, Michl P, Fensterer H, Weimer M, Gansauge F, Leder G, Adler G, Gress TM. Biglycan is overexpressed in pancreatic cancer and induces G1-arrest in pancreatic cancer cell lines. *Gastroenterology.* 2001;121:657–667.
28. Kikuchi A, Tomoyasu H, Kido I, Takahashi K, Tanaka A, Nonaka I, Iwakami N, Kamo I. Haemopoietic biglycan produced by brain cells stimulates growth of microglial cells. *J Neuroimmunol.* 2000;106:78–86.
29. Schaefer L, Beck KF, Raslik I, Walpen S, Mihalik D, Micegova M, Macakova K, Schonherr E, Seidler DG, Varga G, Schaefer RM, Kresse H, Pfeilschifter J. Biglycan, a nitric oxide-regulated gene, affects adhesion, growth and survival of mesangial cells. *J Biol Chem.* 2003;278:26227–26237.
30. Fischer JW, Kinsella MG, Levkau B, Clowes AW, Wight TN. Retroviral overexpression of decorin differentially affects the response of arterial smooth muscle cells to growth factors. *Arterioscler Thromb Vasc Biol.* 2001;21:777–784.
31. Schonherr E, Levkau B, Schaefer L, Kresse H, Walsh K. Decorin-mediated signal transduction in endothelial cells. Involvement of Akt/protein kinase B in up-regulation of p21(WAF1/CIP1) but not p27(KIP1). *J Biol Chem.* 2001;276:40687–40692.
32. Fischer JW, Kinsella MG, Clowes MM, Lara S, Clowes AW, Wight TN. Local expression of bovine decorin by cell-mediated gene transfer reduces neointimal formation after balloon injury in rats. *Circ Res.* 2000;86:676–683.
33. Giri SN, Hyde DM, Braun RK, Gaarde W, Harper JR, Pierschbacher MD. Antifibrotic effect of decorin in a bleomycin hamster model of lung fibrosis. *Biochem Pharmacol.* 1997;54:1205–1216.
34. Border WA, Noble NA, Yamamoto T, Harper JR, Yamaguchi Y, Pierschbacher MD, Ruoslahti E. Natural inhibitor of transforming growth factor-β protects against scarring in experimental kidney disease. *Nature.* 1992;360:361–364.

Available online at www.sciencedirect.com
SCIENCE DIRECT®
Biochemical and Biophysical Research Communications 328 (2005) 288–291
BBRC
www.elsevier.com/locate/ybbrc

Leukemia inhibitory factor induces multi-lineage differentiation of adult stem-like cells in kidney via kidney-specific cadherin 16

Keiichi Hishikawa[a,b,*], Takeshi Marumo[a,b], Shigeki Miura[a], Asato Nakanishi[a], Yumi Matsuzaki[c,g], Katsunori Shibata[a], Hiroko Kohike[c,g], Takuya Komori[c,g], Matsuhiko Hayashi[d], Toshio Nakaki[e], Hiromitsu Nakauchi[f], Hideyuki Okano[c,g], Toshiro Fujita[a,b]

[a] *Department of Clinical Renal Regeneration, Graduate School of Medicine, University of Tokyo, Japan*
[b] *Department of Internal Medicine, Division of Nephrology and Endocrinology, University of Tokyo, Japan*
[c] *Department of Physiology, Keio University School of Medicine, Japan*
[d] *Department of Internal Medicine, Keio University School of Medicine, Japan*
[e] *Department of Pharmacology, Teikyo University School of Medicine, Japan*
[f] *The Institute of Medical Science, University of Tokyo, Japan*
[g] *Core Research for Evolutional Science and Technology (CREST), Japan Science and Technology Corporation, Japan*

Received 23 December 2004
Available online 7 January 2005

Abstract

Side population (SP) is reported to be a stem cell-rich population. In the presence of leukemia inhibitory factor (LIF), cultured kidney SP cells differentiated into multi-lineage in collagen gel but not in synthesized polymer that has no cell adhesion factor. In cultured kidney SP cells, gene expression of kidney-specific cadherin 16 was specifically upregulated in collagen gel but not in synthesized polymer. Moreover, decreasing cadherin 16 expression using siRNA abolished LIF-induced multi-lineage differentiation of kidney SP in collagen gel. These results indicated that LIF induced multi-lineage differentiation of adult stem-like cells in kidney via cadherin 16.

Keywords: Stem cell; Regenerative medicine; Cadherin 16

Existence of adult stem cells is reported in various kinds of tissues, and the so-called side population (SP) is reported to be a stem cell-rich population [1–4]. SP cells exist in various kinds of tissues [5], but the mechanism of multi-lineage differentiation has not been clarified for each type of tissue-derived SP cell, especially in the kidney [6]. In this study, we cultured kidney SP cells both in type I collagen gel and thermoreversible gelation polymer (TGP) that has no cell adhesion factor, and compared differentiation of the cells. Leukemia inhibitory factor (LIF) induced multi-lineage differentiation of kidney SP cells in collagen gel but not in TGP. To clarify the key adhesion factor that determined LIF-induced multi-lineage differentiation of kidney SP cells, DNA microarray analysis was performed. Microarray analysis clarified that kidney-specific cadherin 16 [7] was specifically upregulated in collagen gel but not in TGP. Finally, we examined the role of cadherin 16 in LIF-induced multi-lineage differentiation of kidney SP cells by decreasing cadherin 16 expression using siRNA. Our results showed that cell adhesion factor such as cadherin 16 is required to induce multi-lineage differentiation of adult stem-like cells such as SP cells in the kidney.

* Corresponding author. Fax: +81 3 5800 9738.
E-mail address: hishikawa-tky@umin.ac.jp (K. Hishikawa).

0006-291X/$ - see front matter © 2005 Elsevier Inc. All rights reserved.
doi:10.1016/j.bbrc.2004.12.167

Materials and methods

SP cell sorting and culture. C57/B6 mice (8 weeks of age) were purchased from Clea Japan (Tokyo, Japan). All the procedures described here were approved by the Animal Committee of the University of Tokyo. Mice were anesthetized and perfused via the abdominal aorta with normal saline. The kidneys were harvested and the tissue was minced with a razor blade and digested with collagenase. The cell suspensions were filtered through a cell-strainer (Falcon 2350) to remove debris. The filtrates were analyzed as previously described [4]. Briefly, reserpine was added at a final concentration of 50 μM [4], and cells were then incubated at 37 °C for 15 min and Hoechst dye was added. Kidney SP cells were isolated using a FACS Vantage (BD Biosciences) for flow cytometric sorting. After FACS sorting, kidney SP cells were cultured on MEF feeder cells (RPMEF-N: Dainippon Pharmaceutical, Osaka, Japan) for 7 days with RES101 medium (Dainippon Pharmaceutical, Osaka, Japan) containing leukemia inhibitory factor (LIF: 10 ng/ml). After pre-culture on MEF feeder cells for 7 days, the kidney SP cells were re-seeded in type I collagen gel (Koken, Tokyo, Japan) or thermoreversible gelation polymer (TGP) with RES101 medium until day 28. TGP was purchased from Mebiol (Tokyo, Japan). In Figs. 2B–D, cells just after FACS sorting were cultured in collagen gel or TGP gel for 48 h in the presence or absence of LIF.

Microarray and real-time PCR analysis. DNA microarray hybridization experiments were performed using Clontech Atlas glass Mouse 3.8 I microarray (BD Biosciences) according to the manufacturer's protocol. The protocol and a complete list of genes can be viewed at http://www.bdbiosciences.com/clontech/techinfo/manuals/index.shtml. The DNA arrays were scanned using GenePix4000A [8]. Quantitative real-time PCR was performed using commercially available TaqMan probes (AQP2: Mm00437575 m1, CD31: Mm00476702 m1, neurofilament: Mm00456201 m1, and GATA4: Mm00464689 m1), and analyzed on an ABI PRISM 7000 sequence detector system (BD Biosciences). Quantitative values were obtained from the threshold PCR cycle number at which an increase in signal associated with exponential growth of the PCR product started to be detected. The relative mRNA levels in each sample were normalized to its GAPDH content.

RNA interference. The siRNA for cadherin 16 (pre-designed siRNA, ID#60533) was purchased from Ambion. Transfection was carried out using Qiagen RNAi Starter Kit. 14.5 ml of 20 mM siRNA and 33.75 ml of transfection reagent were added to a medium in a total volume of 250 ml, and left for 15 min at room temperature to allow the formation of transfection complexes. Subsequently, the mixture was diluted with a type I collagen gel to a total volume of 1 ml, and the FACS sorted kidney SP cells were incubated in the gel with LIF-containing culture medium for 48 h.

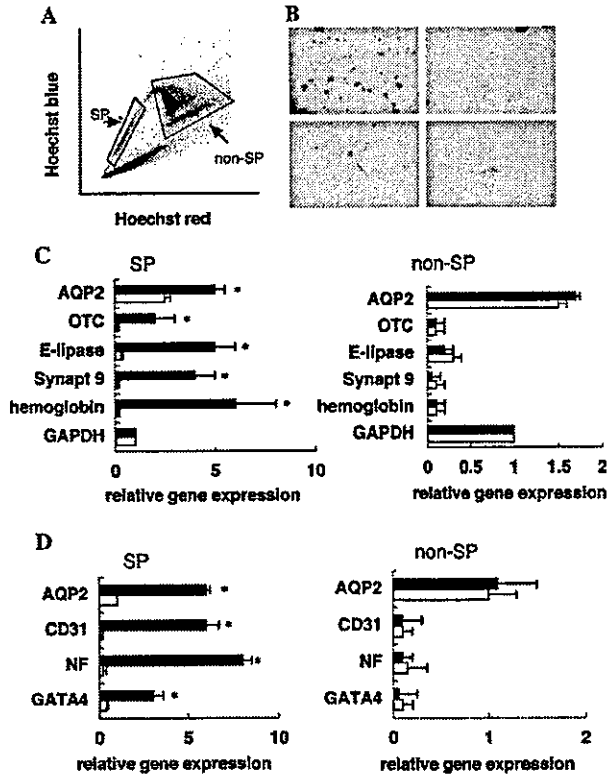

Fig. 1. LIF-induced multi-lineage differentiation of kidney SP cells in collagen gel. (A) Representative FACS profile of SP cells and non-SP cells isolated from the kidney. (B) Representative photographs of cultured kidney SP cells in collagen gel (left upper and lower panels) and TGP gel (right upper) on day 28. Upper panels are low power (40×: phase contrast) and others are high power (400×: phase contrast) photographs. (C) Results of microarray analysis of several lineage-specific genes in cultured kidney SP cells and non-SP cells on day 28 (black bars) compared to day 7 (white bars). Hemoglobin: hemoglobin β-chain, Synapt 9: synaptotagmin, E-lipase: endothelial lipase, OTC: ornithine decarbamylase, and AQP2: aquaporin 2. Expression was normalized to that of GAPDH. Values represent means ± SEM. $^*p < 0.05$ vs. day 7. (D) Results of quantitative PCR of representative genes of three germ layers (ectoderm: NF; mesoderm: CD31, AQP2; and endoderm: GATA4). Closed bars are day 28 and open bars are day 7. Values represent means ± SEM ($n = 4$). $^*p < 0.05$ vs. day 7.

Results

LIF-induced multi-lineage differentiation of kidney SP cells in collagen gel

We isolated whole kidney cells from C57/B6 mice and stained them with Hoechst 33342 dye [9]. The isolated cells were subjected to FACS analysis and immediately used for cell culture (Fig. 1A). Kidney SP cells attached and formed colonies on a mouse MEF feeder layer, and the colonies increased in size until around day 7 but for some reason stopped growing, and then we re-seeded the cells in type I collagen or TGP gel on day 8. On day 28, kidney SP cells formed island-like colonies and tube-like structures in collagen gel (Fig. 1B, left upper panel and lower panels). On the other hand, kidney SP cells never formed such structures in TGP gel not containing cell adhesion factor (Fig. 1B, upper right panel). To examine the multi-lineage differentiation of kidney SP cell in collagen gel and TGP gel, we compared the gene expression of culture SP cells on day 28 with that on day 7 by microarray analysis. Gene expression of several lineage-specific genes such as hemoglobin β-chain [10] (erythrocyte), endothelial lipase [11] (endothelial cell), synaptotagmin [12] (neuron), and ornithine decarbamylase [13] (liver) was very low on day 7, but was significantly upregulated in collagen gel culture on day 28 (Fig. 1C). On the other hand, these genes showed no change in TGP gel culture (Fig. 1C). To examine the

differentiation of kidney SP cells into three germ layers, we performed quantitative real-time PCR analysis of representative genes of the three germ layers (ectoderm: neurofilament (NF); mesoderm: CD31, aquaporin 2 (AQP2); and endoderm: GATA4). In collagen gel culture on day 28, all genes were significantly upregulated as compared to day 7 (Fig. 1D). As in the case with microarray analysis, there was no significant change in gene expression of these genes in TGP gel culture (Fig. 1D).

LIF-induced multi-lineage differentiation was mediated via cadherin 16

To clarify the mechanism of LIF-induced multi-lineage differentiation of kidney SP cells in collagen gel, but not in TGP gel, we tried to clarify the contribution of cell adhesion factors such as cadherins. Compared to TGP gel culture, cadherin 16 was specifically upregulated in collagen gel with LIF on day 28 (Fig. 2A). Next, we examined the effect of LIF on cadherin 16 expression in cultured kidney SP cells by real-time PCR. Treatment with LIF significantly upregulated cadherin 16 in kidney SP cells cultured in collagen gel but not in TGP gel (Fig. 2B). On the other hand, treatment with LIF showed no effect on kidney non-SP cells (Fig. 2B). Finally, we examined whether LIF-induced multi-lineage differentiation is mediated by cadherin 16, we treated kidney SP cells and non-SP cells with siRNA for cadherin 16 and cultured the cells in collagen gel in the presence of LIF. As shown in Fig. 2C, LIF-induced multi-lineage differentiation was significantly inhibited by pre-treatment with siRNA in SP cells. In non-SP cells, LIF alone showed minimum effect and siRNA showed no significant effect (Fig. 2C).

Discussion

Our present results demonstrated that LIF induced multi-lineage differentiation of adult stem-like cells such as SP cells in the kidney via kidney-specific cadherin 16. Cadherin 16 is a unique, tissue-specific member of the cadherin family of cell adhesion proteins that is expressed in the adult kidney and developing genitourinary tract [7,14]. During embryonic development, cadherin 16 is expressed in developing renal tubules in the metanephros and the expression of cadherin 16 is developmentally regulated as well as tissue-specific. Recently, a gene that is homologous to cadherin 16 has been identified in zebrafish, and several studies suggested that cadherin 16 may function as a cell adhesion protein that is required for maintaining tubular integrity [15]. Moreover, Yoshino et al. [16] reported that leukemia inhibitory factor (LIF) is upregulated in ARF, and is considered to play a role for regeneration process. Although the precise functional role of cadherin 16 remains to be determined, our results strongly suggest that cadherin 16 may play an important role in LIF-induced regenerative processes as in developing processes.

TGP gel is a chemically synthesized hydrophilic 3D culture material, which is composed of poly(*N*-isopropylacrylamide-co-*n*-butyl methacrylate) and polyethylene glycol (PEG), and acts as a hydrophilic 3D scaffold without adhesion factors. Recently, we have found that osteogenic differentiation of human mesen-

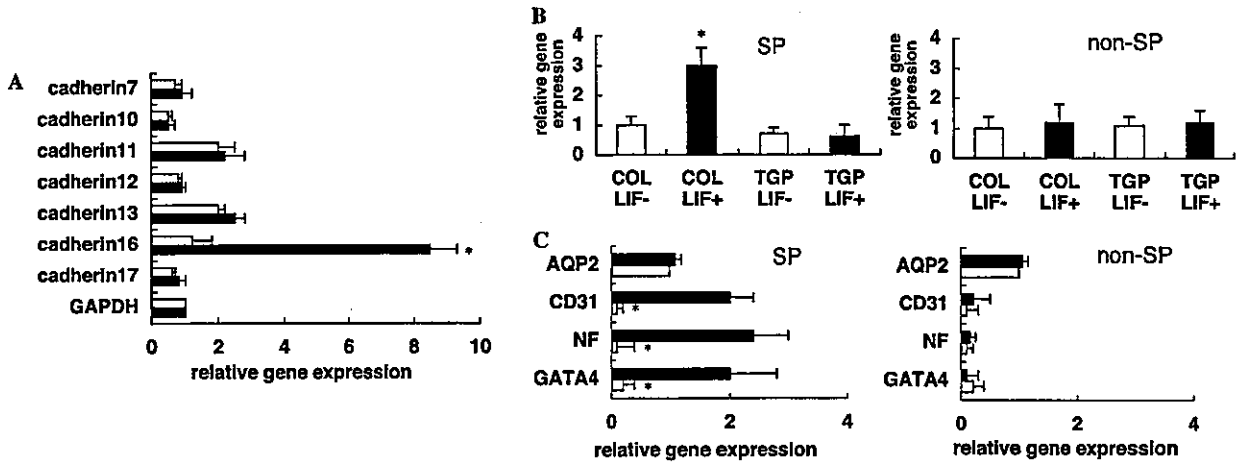

Fig. 2. (A) Microarray analysis of cadherins in cultured kidney SP cells in collagen gel (closed bars) and TGP gel (open bars) on day 28. Average expression levels of each gene were calculated from three independent hybridizations. Expression was normalized to that of GAPDH. Values represent means ± SEM. $^*p < 0.05$ vs. TGP gel. (B) Results of quantitative PCR analysis of cadherin 16 in kidney SP cells and non-SP cells cultured in collagen gel or TGP gel. Values represent means ± SEM ($n = 4$). $^*p < 0.05$ vs. COL LIF. (C) Results of quantitative PCR analysis of representative genes of three germ layers (ectoderm: NF; mesoderm: CD31, AQP2; and endoderm: GATA4). Closed bars are LIF alone and open bars are LIF and siRNA. Values represent means ± SEM ($n = 4$). $^*p < 0.05$ vs. LIF alone.

chymal stem cells (HMSC) was augmented in TGP culture but not in collagen gel [17]. Compared to bone marrow, kidney tissue is rich in extracellular matrix, and this may explain why kidney SP cells required adhesion factors such as cadherin 16 for multi-lineage differentiation. The structure of TGP makes it possible to vary the diffusive speed according to the character of the molecules [17]. TGP may be able to maintain a high local concentration of hydrophobic molecules and hydrophilic large molecules, and this creates a concentration gradient of each molecule. Our results showed that cadherin 16 played key roles in LIF-induced multi-lineage differentiation but it may be possible that TGP may keep high local concentration of LIF-induced unknown factors that can promote multi-lineage differentiation.

Although the physiological function of cadherin 16 is still unclear, the promoter of the mouse cadherin 16 is recently clarified [14,18]. The promoter is TATA-less but contains other consensus promoter elements including an initiator element, GC boxes, and a variant CAAT box as well as potential binding sites for activator protein (AP)-2, hepatocyte nuclear factor (HNF)-1, HNF-3, basic helix–loop–helix (bHLH) proteins, and GATA factors. LIF is a member of the interleukin 6 (IL-6) family and IL-6 induces AP-2 in kidney mesangial cells [19]. These results suggest that LIF may induce cadherin 16 via induction of AP-2 in cultured kidney SP cells in collagen gel.

In summary, our results demonstrated that LIF induced multi-lineage differentiation of adult stem-like cells such as SP cells in the kidney via kidney-specific cadherin 16. These results suggest a new functional role of kidney-specific cadherin 16 in regenerative processes of kidney disease.

Acknowledgments

This study was supported by a grant from the Open Competition for the Development of Innovative Technology and Mochida Pharmaceutical Co. Ltd.

References

[1] M.A. Goodell, K. Brose, G. Paradis, A.S. Conner, R.C. Mulligan, Isolation and functional properties of murine hematopoietic stem cells that are replicating in vivo, J. Exp. Med. 183 (1996) 1797–1806.

[2] S. Zhou, J.J. Morris, Y. Barnes, L. Lan, J.D. Schuetz, B.P. Sorrentino, Bcrp1 gene expression is required for normal numbers of side population stem cells in mice, and confers relative protection to mitoxantrone in hematopoietic cells in vivo, Proc. Natl. Acad. Sci. USA 99 (2002) 12339–12344.

[3] S.M. Majka, K.A. Jackson, K.A. Kienstra, M.W. Majesky, M.A. Goodell, K.K. Hirschi, Distinct progenitor populations in skeletal muscle are bone marrow derived and exhibit different cell fates during vascular regeneration, J. Clin. Invest. 111 (2003) 71–79.

[4] Y. Matsuzaki, K. Kinjo, R.C. Mulligan, H. Okano, Unexpectedly efficient homing capacity of purified murine hematopoietic stem cells, Immunity 20 (2004) 87–93.

[5] A. Asakura, M.A. Rudnicki, Side population cells from diverse adult tissues are capable of in vitro hematopoietic differentiation, Exp. Hematol. 30 (2002) 1339–1345.

[6] H. Iwatani, T. Ito, E. Imai, Y. Matsuzaki, A. Suzuki, M. Yamato, M. Okabe, M. Hori, Hematopoietic and nonhematopoietic potentials of Hoechst(low)/side population cells isolated from adult rat kidney, Kidney Int. 65 (2004) 1604–1614.

[7] R.B. Thomson, P. Igarashi, D. Biemesderfer, R. Kim, A. Abu-Alfa, M. Soleimani, P.S. Aronson, Isolation and cDNA cloning of Ksp-cadherin, a novel kidney-specific member of the cadherin multigene family, J. Biol. Chem. 270 (1995) 17594–17601.

[8] K. Hishikawa, B.S. Oemar, T. Nakaki, Static pressure regulates connective tissue growth factor expression in human mesangial cells, J. Biol. Chem. 276 (2001) 16797–16803.

[9] S. Zhou, J.D. Schuetz, K.D. Bunting, A.M. Colapietro, J. Sampath, J.J. Morris, I. Lagutina, G.C. Grosveld, M. Osawa, H. Nakauchi, B.P. Sorrentino, The ABC transporter Bcrp1/ABCG2 is expressed in a wide variety of stem cells and is a molecular determinant of the side-population phenotype, Nat. Med. 7 (2001) 1028–1034.

[10] W.R. Shehee, D.D. Loeb, N.B. Adey, F.H. Burton, N.C. Casavant, P. Cole, C.J. Davies, R.A. McGraw, S.A. Schichman, D.M. Severynse, et al., Nucleotide sequence of the BALB/c mouse beta-globin complex, J. Mol. Biol. 205 (1989) 41–62.

[11] U. Saxena, M.G. Klein, I.J. Goldberg, Identification and characterization of the endothelial cell surface lipoprotein lipase receptor, J. Biol. Chem. 266 (1991) 17516–17521.

[12] M. Matteoli, K. Takei, M.S. Perin, T.C. Sudhof, P. De Camilli, Exo-endocytotic recycling of synaptic vesicles in developing processes of cultured hippocampal neurons, J. Cell Biol. 117 (1992) 849–861.

[13] Y. Inoue, G.P. Hayhurst, J. Inoue, M. Mori, F.J. Gonzalez, Defective ureagenesis in mice carrying a liver-specific disruption of hepatocyte nuclear factor 4alpha (HNF4alpha). HNF4alpha regulates ornithine transcarbamylase in vivo, J. Biol. Chem. 277 (2002) 25257–25265.

[14] D.A. Whyte, C. Li, R.B. Thomson, S.L. Nix, R. Zanjani, S.L. Karp, P.S. Aronson, P. Igarashi, Ksp-cadherin gene promoter. I. Characterization and renal epithelial cell-specific activity, Am. J. Physiol. 277 (1999) F587–598.

[15] J. Horsfield, A. Ramachandran, K. Reuter, E. LaVallie, L. Collins-Racie, K. Crosier, P. Crosier, Cadherin-17 is required to maintain pronephric duct integrity during zebrafish development, Mech. Dev. 115 (2002) 15–26.

[16] J. Yoshino, T. Monkawa, M. Tsuji, M. Hayashi, T. Saruta, Leukemia inhibitory factor is involved in tubular regeneration after experimental acute renal failure, J. Am. Soc. Nephrol. 14 (2003) 3090–3101.

[17] K. Hishikawa, S. Miura, T. Marumo, H. Yoshioka, Y. Mori, T. Takato, T. Fujita, Gene expression profile of human mesenchymal stem cells during osteogenesis in three-dimensional thermoreversible gelation polymer, Biochem. Biophys. Res. Commun. 317 (2004) 1103–1107.

[18] P. Igarashi, C.S. Shashikant, R.B. Thomson, D.A. Whyte, S. Liu-Chen, F.H. Ruddle, P.S. Aronson, Ksp-cadherin gene promoter. II. Kidney-specific activity in transgenic mice, Am. J. Physiol. 277 (1999) F599–F610.

[19] K. Suyama, Y. Kabuyama, S. Suzuki, Y. Kawasaki, J. Suzuki, H. Suzuki, Y. Homma, Induction of transcription factor AP-2 by cytokines and prostaglandins in cultured mesangial cells, Am. J. Nephrol. 21 (2001) 307–314.

Kidney International, Vol. 67 (2005), pp. 886–896

Osteopontin expression in acute renal allograft rejection

BASSAM ALCHI, SHINICHI NISHI, DAISUKE KONDO, YOSHIKATSU KANEKO, ASAKO MATSUKI, NAOFUMI IMAI, MITSUHIRO UENO, SEITARO IGUCHI, MINORU SAKATSUME, ICHIEI NARITA, TADASHI YAMAMOTO, and FUMITAKE GEJYO

Division of Clinical Nephrology and Rheumatology, Niigata University Graduate School of Medical and Dental Sciences, Niigata, Japan; Blood Purification Center, Niigata University Medical and Dental Hospital, Niigata, Japan; and Department of Structural Pathology, Institute of Nephrology, Niigata University School of Medicine, Niigata, Japan

Osteopontin expression in acute renal allograft rejection.

Background. Osteopontin (OPN) is a potent chemoattractant for mononuclear cells that is up-regulated in various inflammatory states of the kidney. The role of OPN and its expression in human renal allograft rejection are unknown.

Methods. We examined by immunohistochemistry and in situ hybridization, renal biopsies from patients with acute rejection ($N = 22$), protocol biopsies without rejection ($N = 9$), and perioperative donor biopsies ($N = 35$) for intrarenal expression of OPN, and its correlation with clinical, laboratory, and histopathologic parameters. In the rejection biopsies, interstitial monocyte/macrophage infiltration, tubulointerstitial cell proliferation/regeneration and apoptosis were investigated.

Results. In the majority of rejection biopsies, OPN expression by proximal tubular epithelium was widespread, and tended to be enhanced in the tubules surrounded by numerous inflammatory cells. Conversely, in patients that did not experience episodes of rejection and in donor biopsies, OPN expression by proximal tubules was nil or weak. OPN mRNA was colocalized with its translated protein in the renal tubular epithelium. OPN expression positively correlated with the degree of interstitial inflammation ($P < 0.05$), CD68+ monocyte infiltration ($P < 0.01$), Ki-67+ regenerating tubular and interstitial cells ($P < 0.05$ and $P < 0.005$, respectively), but not with terminal deoxynucleotidyl transferase (TdT)-mediated deoxyuridine triphosphate (dUTP) nick-end labeling (TUNEL)-positive apoptotic tubular cells.

Conclusion. These data suggest that inducible expression of OPN in the tubular epithelium may have a pathogenic role in acute renal allograft rejection by mediating interstitial monocyte infiltration and possibly tubular regeneration.

Acute rejection produces significant monocytes accumulation and activation in the graft, which is supposed to be initiated by chemoattractants, including osteopontin (OPN), and has a pivotal role in the pathologic process of rejection, acting directly or in concert with other arms of the immune system.

OPN is a secreted phosphoprotein that has a number of diverse biologic functions, including cell adhesion, migration, and signaling [1–3]. Originally isolated from bone, but is also produced in the kidney, hence, its alternative name uropontin. In rodent and human kidney, OPN is constitutively expressed by distal tubular epithelium [4–6]. OPN is a potent chemotactic molecule for macrophages in vivo [7], and its up-regulated expression by proximal tubular epithelial cells in association with monocyte/macrophage infiltrates has been described in a number of rodent models of renal injury [8–13], and in human renal diseases [14–16]. These studies have suggested that OPN is likely to be a critical mediator of inflammation in specific diseases and injury states.

OPN may also function as a cell survival factor, and may protect cells from undergoing apoptosis [17]. We have previously demonstrated a correlation between up-regulated OPN expression in proximal tubular epithelium and the proliferation and regeneration of tubular epithelial cells during the recovery phase of gentamicin-induced acute tubular necrosis [18]. Similar results have been shown in other toxic models [19] and ischemic/reperfusion models of renal injury [20–22], thereby lending further support for its renoprotective role.

To elucidate the pathogenic significance of OPN and its expression in acute renal allograft rejection, we examined by immunohistochemistry and in situ hybridization, renal biopsies from patients with acute rejection, protocol biopsies without rejection, and perioperative donor biopsies for intrarenal expression of OPN, and its correlation with clinical, laboratory, and histopathologic parameters.

METHODS

Patients

Of 90 consecutive renal transplants performed at Niigata University Hospital over the period (between

Key words: osteopontin, acute rejection, renal allograft, immunohistochemistry, in situ hybridization, donor, protocol, interstitial inflammation, regeneration, apoptosis.

Received for publication June 25, 2004
and in revised form August 31, 2004
Accepted for publication October 11, 2004

May 1996 and August 2002), 32 patients suffered at least one episode of clinical acute rejection in the first year after transplantation. Clinical acute rejection was suspected in cases with acute allograft dysfunction with normal or subtherapeutic levels of calcineurin inhibitors and normal findings by renal ultrasound. Of these, all patients who had undergone a renal biopsy within 7 days of the onset of acute allograft dysfunction with (*1*) pathologically confirmed acute rejection or borderline rejection according to the standardized criteria of Banff working classification of kidney transplant pathology and (*2*) adequate formalin-fixed tissue available for immunohistochemistry were included in this study ($N = 20$). The remaining cases (12 of 32) with clinical acute rejection were excluded because six patients had not undergone a renal allograft biopsy, three patients lacked the minimum criteria for borderline rejection or in whom cyclosporine toxicity was suspected, and three patients lacked adequate tissue to allow the studies described below. At the time of biopsy, 15 out of 20 patients were on triple-drug regimen, including cyclosporine or tacrolimus with mycophenolate mofetil, azathioprine or mizoribine and prednisolone. The other five patients were on dual therapy with tacrolimus and prednisolone. In 11 rejection cases, antirejection treatment was initiated before graft biopsy based on clinical suspicion.

In an attempt to stop steroid in renal transplant recipients with early uncomplicated clinical course, the practice to obtain protocol biopsies was introduced at Niigata University Hospital in January 2003. Until March 2004, 16 protocol biopsies were done. Among them, nine lacked the minimum criteria for borderline rejection, and served as a control group. The immunosuppressive regimen in the control group was comprised of cyclosporine or tacrolimus, mycophenolate mofetil, and prednisolone.

The study also included the perioperative biopsies of transplanted kidneys ($N = 35$) of the same patients with acute rejection, including 15 pairs of preimplantation biopsies and 1-hour postreperfusion biopsies of the same grafts and preimplantation biopsies of five additional grafts. Normal human kidney specimens ($N = 4$) were obtained from normal portions of kidneys resected for localized neoplasms. Biopsies were performed only after obtaining written informed consent from the patients.

Clinical data were gathered from our patient and pathology databases and review of medical records (e.g., age, warm ischemic time, total ischemic time, and immunosuppressive therapy). Serum creatinine level, and urinary protein excretion, of each patient were obtained at the time of biopsy. Additionally, serum creatinine level was obtained at two other points; the maximum serum creatinine within 1 week of renal biopsy, and at 3 months after the biopsy, an arbitrary date set up to signify a stable outcome.

Antibodies

To examine the hypothesis that different molecular forms of OPN, which may have diverse or even contrary functions in normal or pathologic conditions, may be detected by antibodies against different epitopes of OPN, we tried two monoclonal antibodies which recognize different epitopes of human OPN (IBL, Fujioka, Japan). O-17 is a rabbit IgG affinity-purified antibody directed against the N-terminal of human OPN. 10A16 is a mouse IgG1 antibody directed against a mid part of human OPN. Their specific recognition of OPN has been characterized by Western blotting [23]. Both antibodies demonstrated identical patterns of staining, we therefore chose one of these reagents, O-17, because of its specificity against the most active N- terminal fragment which contains the cell-binding arginine-glycine-aspartate (RGD) sequences to perform the immunohistochemical staining in this article.

E29 (Dako, Glostrup, Denmark) is a murine monoclonal IgG2a that is specific for epithelial membrane antigen (EMA). EMA is known to be expressed by distal convoluted tubules, collecting ducts, and the thick ascending limb of the loop of Henle, and was shown to be colocalized with OPN in human adult kidney [4].

PG-M1 (Dako) is a well-characterized murine monoclonal antibody directed against the CD68 epitope present on human monocytes and macrophages.

MIB-1 (Dako) is a well-established murine monoclonal antibody for the demonstration of Ki-67 antigen, a nuclear protein preferentially expressed during cell proliferation [24].

Immunohistochemistry

Serial sections of formalin-fixed, paraffin-embedded biopsies of 3 μm thickness were prepared. For immunohistochemistry to detect OPN, the sections were first deparaffinized and rehydrated, they were then heated in a 0.01 mol/L citrate buffer (pH 6) under microwave (5 minutes × 2) to unmask antigenicity. Subsequently, they were treated with normal goat serum (Chemicon, Temecula, CA, USA) at room temperature for 30 minutes to block nonspecific binding, and incubated with the primary antibody, O-17 at a dilution of 1:50 over night at 4°C. After washing with phosphate-buffered saline (PBS), OPN was detected using alkaline phosphatase enhanced detection kit (red) (Ventana Medical Systems, Tucson, AZ, USA).

Double immunohistochemistry was performed to detect OPN in combination with EMA, Ki-67 and CD68. Briefly, the sections were treated once more in a microwave oven, immersed in 3% H_2O_2 in methanol to block the residual endogenous peroxidase, and in case of CD68, incubated with trypsin (Wako Pure Chemical Industries, Osaka, Japan) for 30 minutes at 37°C. They were sequentially incubated with normal goat serum,

the primary antibody; either E29 (1:100), MIB-1 (1:50), or PG-M1 (1:1) overnight at 4°C, biotinylated goat antimouse secondary antibody, and the avidin-biotin-peroxidase [horseradish peroxidase (HRP)] complex (Ventana Medical Systems). The sections were then visualized with 3, 3′- diaminobenzidine (DAB) Dako, Carpinteria, CA, USA) to give a brown reaction product. The cellular nuclei of the sections were counterstained with hematoxylin, overslipped, and examined under light microscopy.

Detection of apoptotic cells

Rejection specimens were examined for apoptosis using terminal deoxynucleotidyl transferase (TdT)-mediated deoxyuridine triphosphate (dUTP) nick-end labeling (TUNEL) of fragmented DNA as described by Gavrieli, Sherman, and Ben-Sasson [25]. DNA labeling was performed using the TACS (Trevigen Apoptotic Cell System) 2 TdT/DAB kit for apoptosis detection in situ. Details are found in manufacturer's instructions (Trevigen, Gaithersburg, MD, USA). Briefly, paraffin-embedded sections were deparaffinized in xylene, rehydrated through graded concentration of ethanol, and washed with PBS for 10 minutes. To facilitate the penetration of enzymes and biotinylated deoxyuridine, the slides were subjected to 30 minutes of proteinase K (10 μg/mL) digestion, and washed in deionized water two times for 2 minutes. Endogenous peroxide was quenched by immersion in 3% H_2O_2 in 40% methanol for 5 minutes. Then, the sections were rinsed in TdT labeling buffer, incubated in the TdT labeling mixture at 37°C for 1 hour. The reaction was stopped and the sections were washed with PBS two times for 2 minutes. They were subsequently covered with peroxidase-labeled streptoavidin for 15 minutes, washed in PBS to remove unbound conjugate, and finally stained with DAB-H_2O_2 solution. Sections were counterstained with methyl-green for 1 minutes, and coverslips were mounted.

To confirm the staining specificity, the TUNEL procedure was modified as follows; for the positive controls, TACS-Nuclease was added to the labeling mix to generate DNA break in every cell. Negative controls included omission of TdT from buffer solution.

In situ hybridization

To amplify cDNA of human OPN coding region (903 bp) by polymerase chain reaction (PCR), two primers, 5′-ATGAGAATTGCAGTGATTTGC-3′ as a forward primer and 5′-CGTAGAAGACTCCAGTTAA TT-3′ as a reverse primer, were used. The PCR product was cloned into a pGEM-T cloning vector (Promega, Madison, WI, USA). The template was subsequently digested with *Nde*I, and ligated with T4-ligase to obtain OPN cDNA of 481 bp (from 422 to 903 bp).

The plasmid sample with the OPN cDNA (481 bp) was linearized with *Nco*I as a sense probe and *Nde*I as an antisense probe, respectively. In vitro transcription of the cDNA was done using a digoxigenin (DIG) RNA labeling kit (SP6/T7) (Roche Diagnostics, Penzberg, Germany). 500 ng of linearized plasmid was used as a template and incubated with T7 DNA-dependent RNA polymerase for 2 hours to obtain an antisense probe. A SP6 promoter was used to produce a sense probe, which was used as a negative control.

In situ hybridization was done by the automated mRNA in situ hybridization application (Ventana Medical System) as described in [26]. Briefly, serial sections were automatically deparaffinized, fixed, and acid treated. Then, the tissue sections were subjected to cell conditioning and protease digestion. Hybridization was performed with DIG-labeled OPN antisense probe (30 ng/slide) at 60 for 6 hours, followed by incubation with an alkaline phosphatase-conjugated anti-DIG antibody (Roche Diagnostics) at 37°C for 1 hour, and the signal was detected using a nitro blue tetrazolium chloride 5-bromo-4-cloro-3-indolyl phosphate toluidine salt (NBT/BCIP) substrate solution for 3 hours.

Quantitative analysis

All counts and pathologic evaluations were performed on coded slides without prior knowledge of the clinical or histologic diagnosis. In each section, all fields of the renal cortex were counted on a 1 cm^2 eyepiece graticule with 10 × 10 equidistant squares. Under high magnification (×400), a minimum of 10 and a maximum of 20 consecutive nonoverlapping fields per section were counted (average measured area, 3.5 ± 0.75 mm^2). On double-staining sections, the percentage area of OPN-positive proximal (EMA-negative) and nonproximal (EMA-positive) tubular cell segments in the total area of proximal and nonproximal tubules were calculated, while the squares falling on glomeruli, Bowman's capsules, interstitium, or tubular lumen were excluded. In addition, the intensity of staining in proximal tubular segments was graded semiquantitatively, as described previously [27], with a scale of 0, no staining; 1+, weak staining; 2+, moderate staining; and 3+, strong staining, comparable to the observed intensity of staining in distal tubular segments.

On separate serial sections, the quantification for CD68-positive, Ki-67–positive, and apoptotic cells was undertaken. Under high magnification (×400) equivalent numbers of cortical graticule fields per section were examined, and the data are presented as the average number of CD68-positive cells per field; the percentage of Ki-67–positive tubular and interstitial cells relative to the total number of tubular and interstitial nuclei, respectively, and as the percentage of apoptosis-positive

Table 1. Baseline characteristics of the transplant recipients[a]

	Acute rejection ($N = 20$)	No rejection ($N = 9$)
Age *years*	34.7 ± 12.5	41.6 ± 13.2
Gender *Male/female*	15/5	5/4
Donor *living/cadaver*	19/1	9/0
Warm ischemic time *minutes*	6.7 ± 3.1	5.0 ± 1.3
Total ischemic time *minutes*	111.3 ± 101.1	94.9 ± 39.8
Number of biopsies/patients	22/20	9/9
Biopsy time *days after transplantation*	68.0 ± 83.2	55.0 ± 71.9
Serum creatinine at biopsy *mg/dL*	2.1 ± 1.9	1.2 ± 0.7
Maximum serum creatinine within a week of renal biopsy *mg/dL*	2.5 ± 2.3	NA
Serum creatinine 3 months after biopsy *mg/dL*	1.6 ± 0.8	1.1 ± 0.9
Urine protein at biopsy *g/day*	0.3 ± 0.3	0.2 ± 0.2
Banff category	Borderline = 11	<Borderline = 9
IA	7	
IB	4	

NA is non applicable.
[a]Plus-minus values stand for means ± SD were not significantly different between the two groups.

tubular cells. The correlation analysis for OPN and CD68 or Ki-67 was undertaken on double-staining immunohistochemistry sections for OPN protein and either CD68 or Ki-67 antigen.

Statistical analysis

Results were analyzed by a commercial software package, SPSS 11.5 for Windows. We used unpaired Student *t* test, Mann-Whitney U test, Kruskal-Wallis H test, Wilcoxon single-rank test, and linear regression analysis, as appropriate. *P* values less than 0.05 were used as the criteria of statistically significant differences.

RESULTS

Table 1 shows the clinical profile of patients with acute rejection versus control group. There was no significant difference between the two groups with regards to age, duration of ischemia, time of biopsy, serum creatinine, and urinary protein. As for the donors, there were five males and 15 females, aged 55.6 ± 10.8 years.

Expression of OPN protein and mRNA

To characterize the renal tubular epithelium, we carried out double immunohistochemistry for OPN and EMA as a marker of distal tubule. All renal biopsies ($N = 70$), including acute rejection, protocol, perioperative and normal biopsies, were scored for both the percentage of OPN-positive tubular area and the intensity of OPN immunostaining. Distal tubules served as an internal control for OPN immunostaining, as they constitutively express OPN protein, and did so in many, but not all, segments of the distal nephron in every tissue studied.

In our study, all of the 22 rejection biopsies showed tubulitis with interstitial infiltration but no vasculitis. The high number of borderline rejections ($N = 11$) is probably because many of those biopsies were obtained after antirejection treatment was initiated so that inflammatory changes may have diminished in individuals that did indeed have a significant rejection episodes [28].

In the majority of rejection biopsies that we examined, OPN expression by the proximal tubular epithelium was widespread, exhibited low-to-moderate signal intensity, and was predominantly observed in a distinct perinuclear pattern. The intensity of OPN immunostaining was remarkably high in the degenerated proximal tubular cell segments and in the tubules surrounded by numerous inflammatory cells. In addition, a few number of the infiltrating cells within the interstitium demonstrated positive OPN expression. Glomerular OPN expression was occasionally observed within the glomerular tuft and in the parietal epithelial cells lining Bowman's capsule. Two representative cases are shown in Figures 1A, and 2.

Quantitative analysis showed that OPN-positive area in the rejection biopsies was significantly higher than that of protocol, preimplantaion, postreperfusion, and normal biopsies, in both proximal and distal tubules. The signal intensity of OPN expression by proximal tubules, a rough measure of the amount of protein present, was significantly higher in the rejection biopsies when compared with that of the other groups (Fig. 3), suggesting that OPN expression was induced in the proximal and distal tubular epithelium in acute rejection.

Regression analysis showed no significant correlation between OPN expression and any of the three levels of serum creatinine, as outlined in the **Methods** section, or with the level of urinary protein excretion (rho = 0.05; $P > 0.05$). Although no correlation could be found between OPN expression and the pathologic grade of rejection, OPN expression by proximal tubules significantly correlated with the extent of interstitial inflammation but not with tubulitis (Fig. 4). There were no significant differences in the tubular expression of OPN, between biopsies from patients receiving cyclosporine ($N = 8$) or tacrolimus ($N = 12$) as a maintenance immunosuppressive therapy, or between biopsies from those with and without prior antirejection treatment.

The protocol biopsies used in this study had no prominent mononuclear inflammatory cell infiltrate or tubulitis. The perioperative biopsies generally had no specific pathologic abnormality except for the cadavaric biopsy specimen which showed features of acute tubular necrosis.

In the protocol and perioperative biopsies, OPN was uniformly expressed at high intensity by a subset of distal tubules, whereas no or weak expression of OPN by proximal tubules (Fig. 1C). Quantitative analysis showed

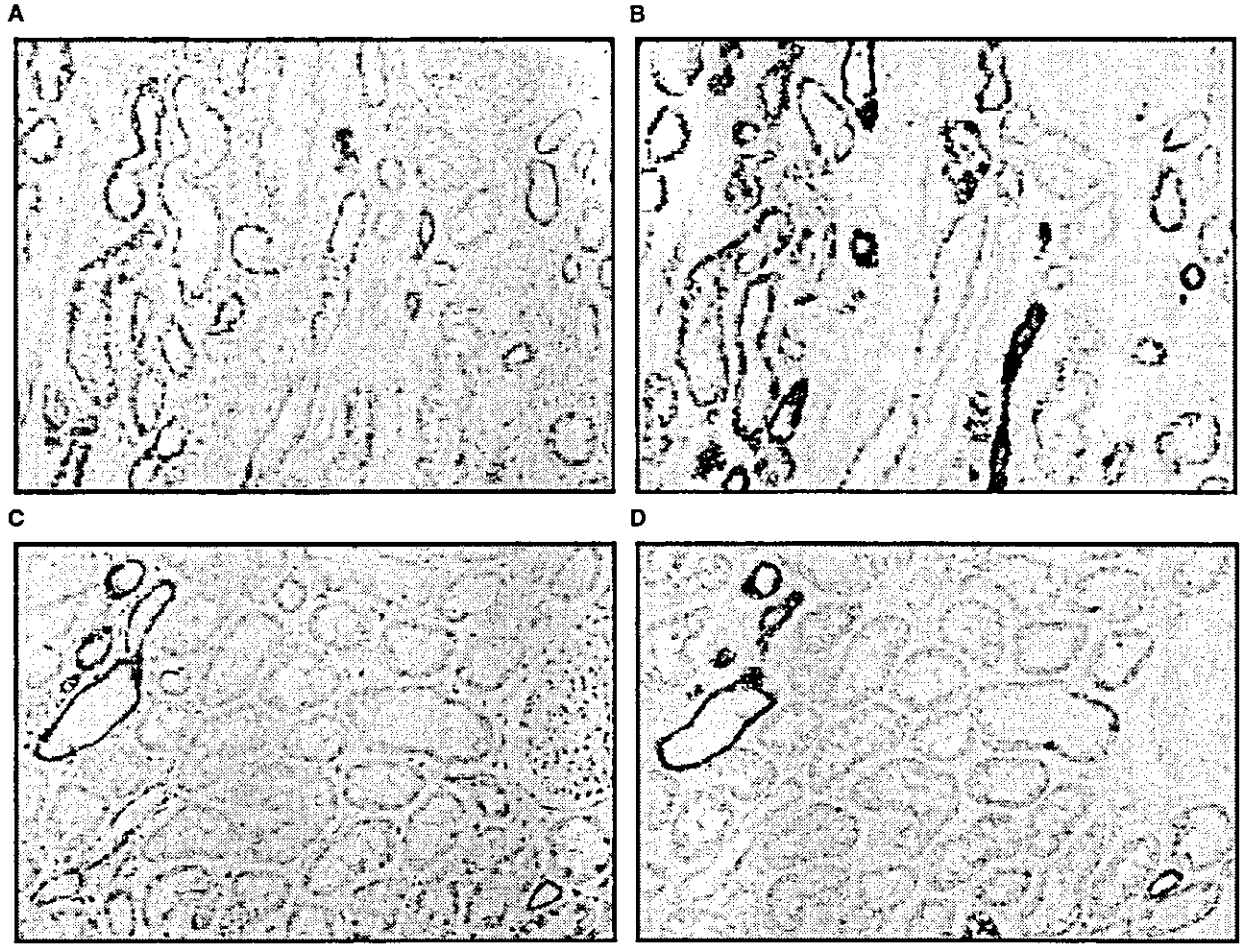

Fig. 1. Replicate tissue sections. (*A* and *B*) Sections with acute rejection demonstrating the colocalization of osteopontin (OPN) protein and mRNA by immunohistochemistry and in situ hybridization. OPN protein is visualized by alkaline phosphatase (red) and OPN mRNA is hybridized with digoxigenin-labeled OPN antisense probe. There is widespread expression of OPN by both proximal and distal tubules. Glomerular OPN expression can be seen within the glomerular tuft and in the parietal epithelial cells lining Bowman's capsule. (*C* and *D*) Sections from a protocol biopsy without rejection showing OPN protein expression generally confined to the distal tubules, corresponding to the patterns of OPN synthesis by in situ hybridization (magnification ×66).

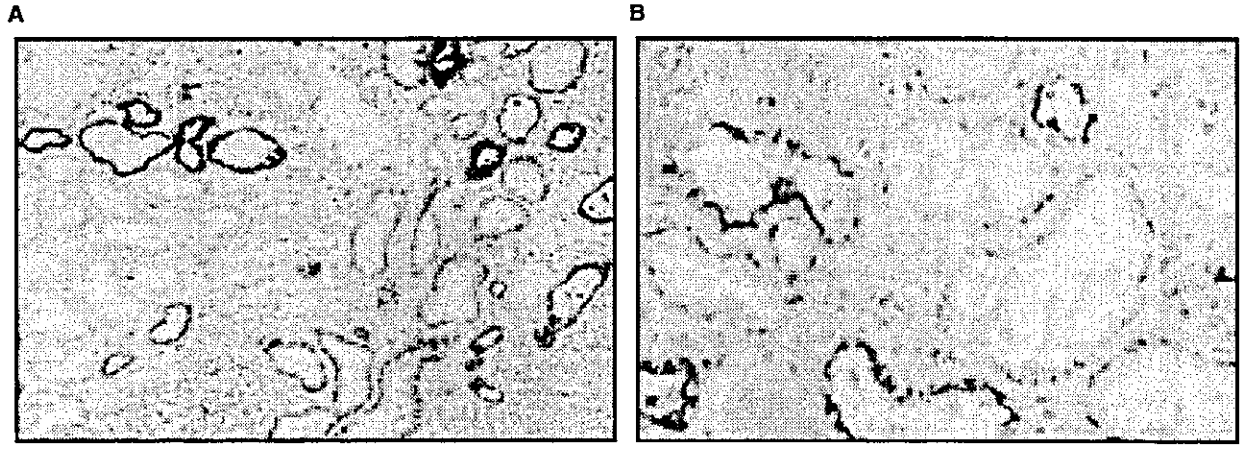

Fig. 2. Double immunohistochemistry. (*A*) Osteopontin (OPN) (red), and epithelial membrane antigen (EMA) (brown) in a rejection specimen, demonstrating strong OPN expression in the tubular segments surrounded by numerous inflammatory cells. (*B*) Higher power view of the same kidney (A), demonstrating the distinct perinuclear staining pattern of OPN [magnification ×66 (A) and ×160 (B)].

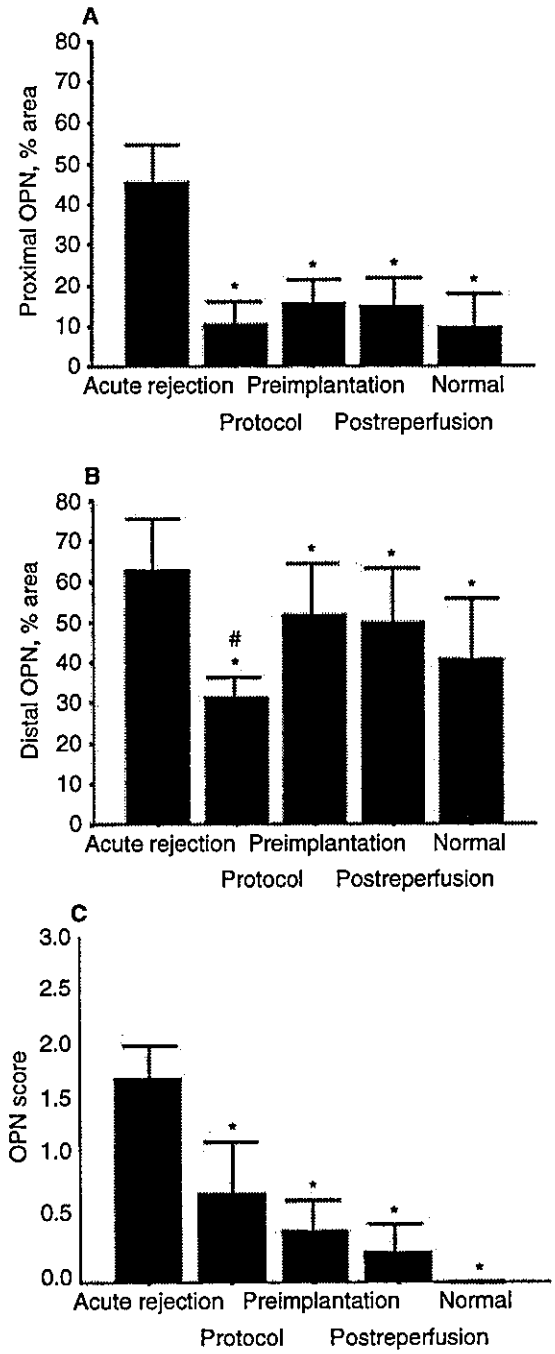

Fig. 3. Quantitative analysis of osteopontin (OPN) expression. (*A*) Proximal [epithelial membrane antigen (EMA)-negative] tubules. (*B*) Distal (EMA-positive) tubules. (*C*) OPN score in acute rejection (N = 22), protocol (N = 9), preimplantation (N = 20), postreperfusion (N = 15), and normal biopsies (N = 4). *P < 0.05 versus acute rejection; #P < 0.05 versus preimplantation and postreperfusion.

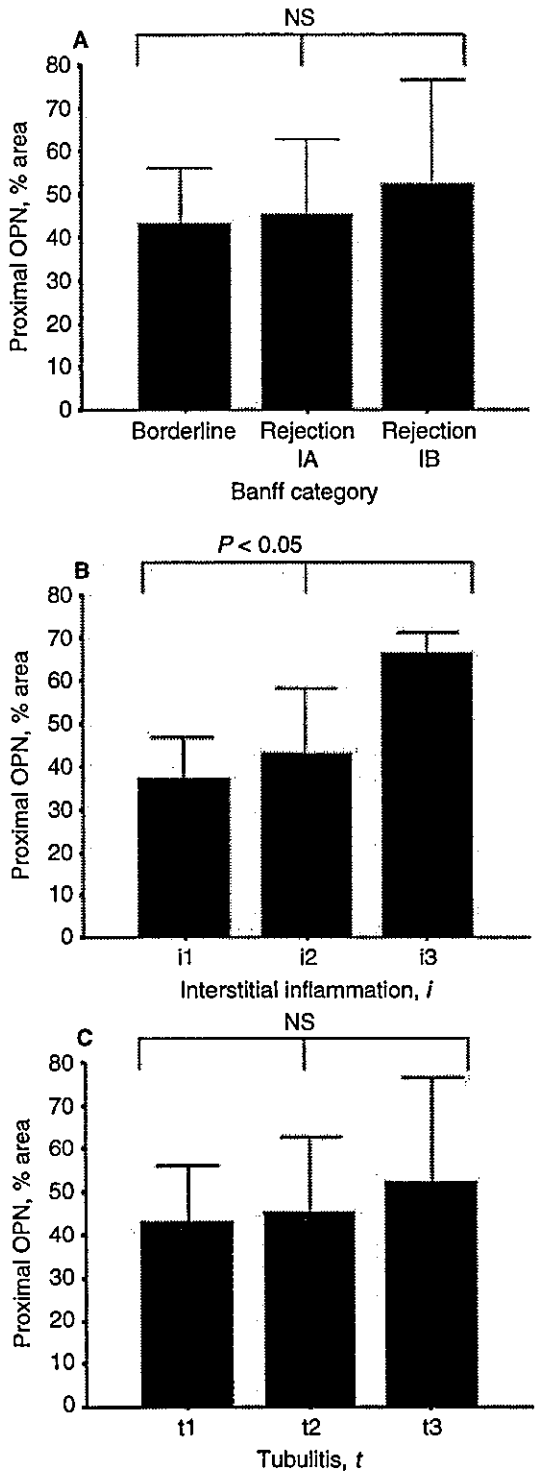

Fig. 4. Quantitative analysis shows OPN expression. (*A*) Expression is not associated with the pathological grade of rejection. (*B*) Expression is significantly correlated with the degree of interstitial inflammation. (*C*) Expression is not correlated with tubulitis. NS is not significant.

that OPN-positive area in proximal tubules was not significantly different between protocol, perioperative, or normal biopsies. OPN-positive area in distal tubules was indeed significantly lower in the protocol biopsies when

compared with that of perioperative biopsies but not with normal biopsies (Fig. 3B).

In the perioperative biopsies, regression analysis between OPN expression and donor age did not show a significant correlation. There was also no correlation between warm ischemic time and OPN expression in preimplantation biopsies or between total ischemic time and OPN expression in postreperfusion biopsies.

To confirm the colocalization of OPN, protein and mRNA replicate sections for immunohistochemistry and in situ hybridization were used. In all sections that we examined, results of in situ hybridization for OPN mRNA expression closely mirrored those seen by immunohistochemistry. As can be seen in Figure 1, the patterns of localization of OPN protein and mRNA were very similar. All sections examined with a sense probe were negative.

Correlation of OPN expression and macrophage infiltrate

To examine the relationship between OPN and monocyte/macrophage infiltration in acute rejection, we performed immunohistochemistry for CD68 and double-staining for OPN and CD68. In many cortical areas CD68-positive cells tended to be localized in close proximity with tubular segments that demonstrated positive OPN expression (Fig. 5A). The quantitative data on the extent of interstitial macrophage infiltration and OPN expression present in the rejection specimens used for this study are presented as a scattergram in Figure 5B. In individual tissue section, the area of OPN-positive tubular segments positively correlated with the degree of interstitial macrophage accumulation (rho = 0.546; $P < 0.01$).

Demonstration of Ki-67–positive cellular nuclei and its relationship with OPN

To clarify the relationship between OPN expression and cellular proliferation/regeneration, we carried out immunohistochemistry for Ki-67 and double-staining for OPN protein and Ki-67 antigen. Rejection biopsies were scored independently for the percentage of Ki-67–positive tubular and interstitial cells. In almost all acute rejection specimens that we examined, Ki-67–positive tubular cells were rare (mean 1.4%; range 0% to 6.3%), whereas Ki-67–positive interstitial cells varied considerably from 0.2% to 27% (mean 8.3%). Regression analysis showed that the number of Ki-67–positive tubular epithelial and interstitial cells was associated significantly with OPN expression by proximal tubules (rho = 0.529, 0.639; and $P < 0.05$, < 0.005, respectively) (Fig. 6A and B). The result of double-staining, however, demonstrated that the location of OPN expression had no distinct relationship with that of tubular or interstitial cell proliferation in most areas, but in some areas; the Ki-67–positive cells were observed within or in the vicinity of OPN-positive tubules (Fig. 6C).

Demonstration of cellular apoptosis and its relationship with OPN

Apoptotic cells were detected in the tubular epithelia in 18 cases of acute rejection (82%), with an overall rate of 2.5%, and range of 0% to 10.6%. TUNEL-positive cells were almost exclusively observed in the distal tubular epithelial cells (Fig. 7), in contrast apoptosis was very rare in the proximal epithelial cells. Apoptosis was occasionally seen in the interstitial and glomerular compartment. There was no significant correlation between TUNEL-positive tubular cells and the extent of OPN expression by either proximal or distal tubules. No correlation could be found between TUNEL-positive tubular cells and the extent of allograft dysfunction or the pathologic grade of rejection.

DISCUSSION

OPN is well-known as a mediator of tubulointerstitial injury that accompanies glomerulonephritis [7, 8, 14–16]; whereas its significance in renal allograft rejection remains elusive. The present study clearly indicated that OPN (protein and mRNA) expression significantly enhanced in acute rejection, and was correlated with interstitial inflammation, macrophage infiltration, and cellular proliferation but not with apoptosis.

Hudkins et al [27] [abstract; Hudkins KL, *J Am Soc Nephrol* 11:A3497, 2000] found strong OPN protein and mRNA expression by tubular epithelium in pretransplant biopsies and in biopsies with cyclosporine toxicity without an inflammatory cell infiltration, though the number of donor biopsies available in their study was too small to calculate a correlation.

The strong OPN expression in donor biopsies has been assumed to be caused by ischemia, a known factor to induce OPN expression in renal proximal tubular epithelium [21, 29]. However, no data were available on the association between the duration of ischemia and the level of OPN expression.

In this study, we found no or weak expression of OPN protein and mRNA by proximal tubules in the majority of perioperative donor biopsies, and was independent to the ischemic time. This is simply because almost all of the studied donor biopsies, in contrast with those by Hudkins et al [27], were from living donors; therefore, the ischemic time was generally short. Constitutive expression of OPN by distal tubules was significantly higher in the perioperative donor biopsies as compared with that of protocol biopsies. This finding is unlikely to be attributable solely to the fact that constitutive OPN expression by distal tubules varies widely in human adult

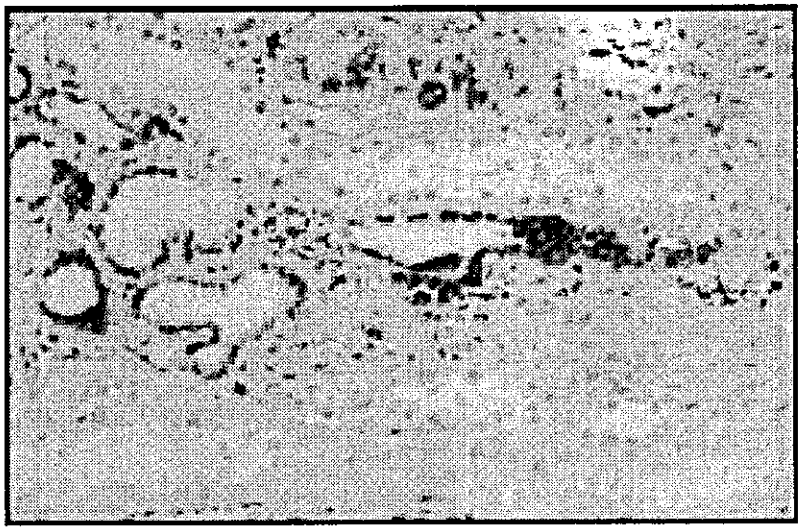

Fig. 5. Double immunohistochemistry. (*A*) Osteopontin (OPN) (red) and CD68+ macrophage (brown) in renal graft with acute rejection, demonstrating the CD68+ macrophages in close proximity with tubules expressing OPN (magnification ×100). (*B*) Regression analysis showed OPN expression in patients with acute rejection significantly correlated with CD68+ monocyte infiltration of adjacent interstitium.

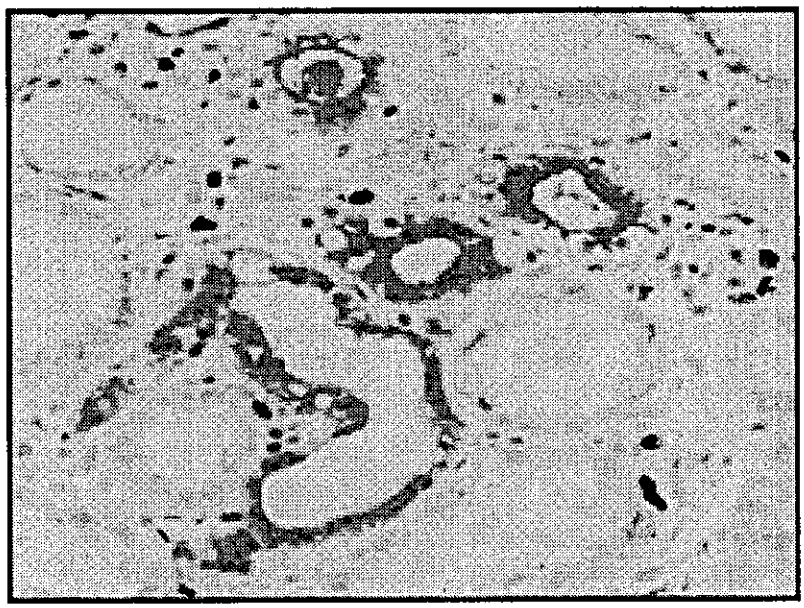

Fig. 6. Regression analysis shows significant correlation between osteopontin (OPN) expression. (*A*) Ki-67+ tubular cells, (*B*) Ki-67+ interstitial cells in patients with acute rejection. (*C*) Demonstrative case of acute rejection showing the location Ki-67+ cells (brown) was related to tubular OPN expression (red) in some areas (magnification ×100).

kidney [4]. Although no significant correlation could be found between ischemia time and the level of OPN expression by distal tubules in the donor biopsies, it is likely that the ischemia/reperfusion which might preferentially induce OPN in the distal tubules. In a rat model of renal ischemia, it has been shown that OPN expression by distal tubules rapidly increased, as it was already highly significant 12 hours after reperfusion, whereas proximal tubules showed a delayed response [21].

In the majority of rejection biopsies that we examined, the presence of increased OPN immunostaining that was accompanied by a concomitant OPN mRNA up-regulation, not only in distal but also in proximal tubular cells indicate OPN gene induction in these cells with a possible role of OPN in acute rejection.

As the hallmark of acute rejection is tubulointerstitial inflammation, we hypothesize that some intrarenal proinflammatory cytokines act via autocrine/paracrine mechanism to stimulate OPN gene transcription and expression. The consistently observed up-regulation of OPN in areas of cellular infiltrate supports this hypothesis. Classic mediators of acute inflammation such as tumor necrosis factor-α (TNF-α), and interleukin-1β (IL-1β) strongly induce OPN expression [30, 31]. Cytokine mRNA analysis on human renal allograft biopsies by a PCR-based assay confirmed the presence of

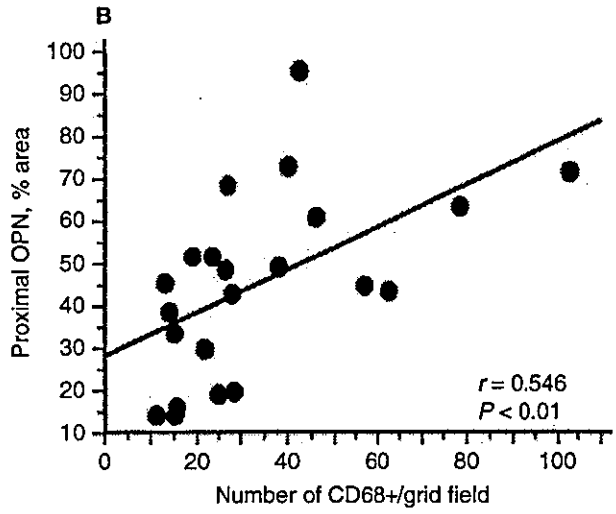

Fig. 5. (continued.)

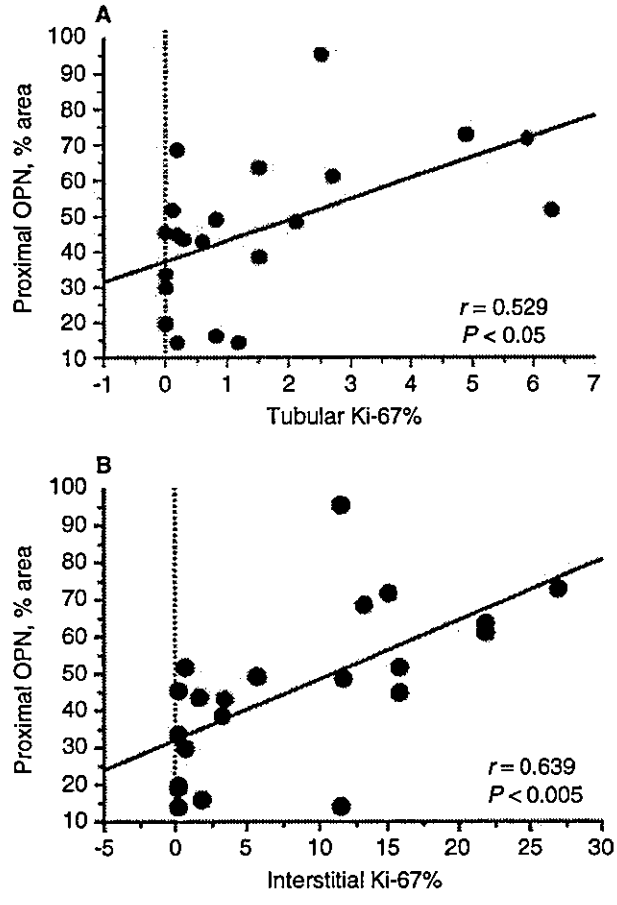

Fig. 6. (continued.)

these two mediators in acute cellular rejection [32], while immunohistochemical studies demonstrate a marked TNF-α expression by infiltrating inflammatory cells and adjacent tubular cells in acute cellular rejection but not in normal kidney [33, 34]. Other potential culprit that can induce OPN up-regulation is endothelin-1 [35], which was shown to be up-regulated on the tubular epithelial cells in acute rejection [36, 37]. Taken together, these observations may explain the high level of OPN expression in acute rejection. Nonetheless, other factors such as ischemia may also be involved.

The Banff working classification of renal transplant pathology only focuses on the cellular inflammatory reactions, including interstitial cell infiltration, tubulitis, and arteritis. However, the extent of tubular cell injury is not fully addressed in this classification. In this study, the degenerated proximal tubular epithelial cells consistently showed strong expression of OPN, suggesting that OPN may have a complementary diagnostic value in assessing the tubular cell injury in acute rejection.

Acute rejection is predominantly a cell mediated process with CD4+ T lymphocytes playing a central role. CD4+ T cells differentiate into two distinct T-helper cell subsets, Th1 or Th2 cells, which have distinct profile of cytokine production and thus mediate distinct functions. Th1 cells are mainly involved in cell-mediated immunity, whereas Th2 cells are associated with humoral immunity [38]. OPN, by reacting with its receptors, influences the polarization of T-helper cells to the Th1 or Th2 phenotypes. OPN integrins interaction enhances Th1 whereas OPN-CD44 interaction inhibits Th2 cytokines expression [39, 40]. Cytokines secreted by the Th1 cells, such as interferon-γ (IFN-γ) and IL-2 play a critical role in graft rejection. Whether OPN directly affects those cytokines in acute rejection in vivo remains to be determined.

The function of OPN in acute rejection appears to extend beyond being merely proinflammatory. Our data showed significant relationship between OPN expression and tubulointerstitial cell proliferation/regeneration, suggesting a possible role of OPN in the repair of tubular injury. However, in contrast with our group's previous experimental model of acute tubular injury [18], double-staining for OPN and Ki-67 antigen did not show a close relationship in most areas. These contrasting results may be explained by the different models and phases of renal injury. In this study, biopsies were taken during the early phase of acute rejection; therefore most of the tubular cells have not yet been regenerating. Indeed most of the Ki-67–positive cells were in the interstitial compartment.

Apoptosis is a cellular phenomenon generally found within rejecting transplant [41]. Although the role and mechanisms of apoptosis during rejection of allograft kidneys are not known, it appears likely that some apoptotic effectors regulate the rejection process. The regulation of antiapoptotic and proapoptotic oncogenes may vary with

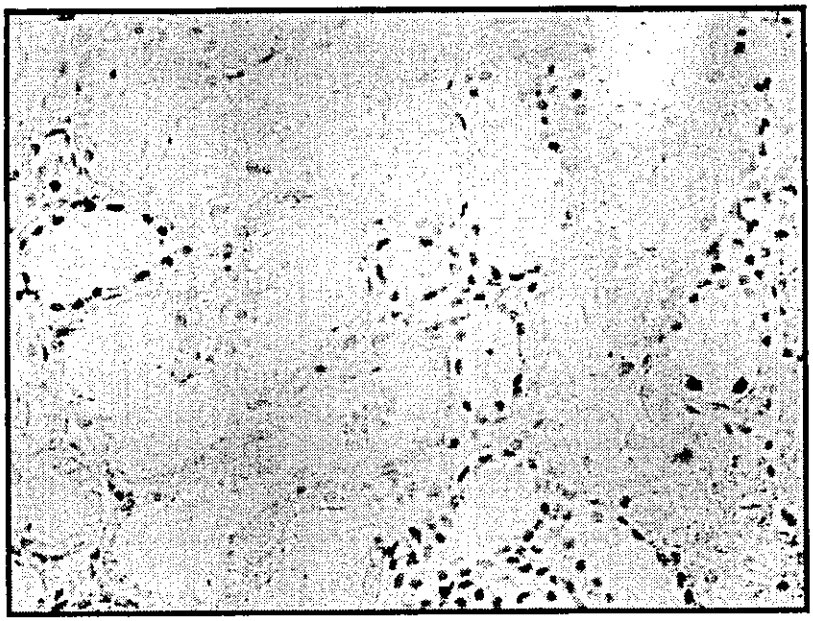

Fig. 7. A tissue section with acute rejection stained with a 2 terminal deoxynucleotidyl transferase (TdT)/3, 3′-diaminobenzidine (DAB) kit for apoptosis detection in situ, and methylene green counterstaining. Terminal deoxynucleotidyl transferase (TdT)-mediated deoxyuridine triphosphate (dUTP) nick-end labeling (TUNEL) + signals (brown) were almost confined to the distal tubules, and were unrelated to interstitial cell infiltration (magnification ×100).

cell types during the acute and recovery phase of acute renal failure [42]. This may account for the frequently observed apoptosis in the distal but not the proximal tubules in acute rejection. OPN has antiapoptotic effect. In a recent study, ischemic kidneys from OPN knockout mice showed significantly enhanced apoptosis [43]. OPN expression did not correlate with the observed number of apoptotic cells, indicating that OPN is probably an irrelevant regulator of apoptosis in acute rejection.

The available data on the significance of OPN expression in human renal diseases are still limited. In IgA nephropathy, OPN has been shown to have a negative impact on the prognosis [16]. In membranous nephropathy, tubular expression of OPN was significantly higher in patients with progressive disease [15]. In these two kinds of chronic glomerulonephritis, the adverse prognostic significance of OPN expression is probably caused by its significant association with interstitial fibrosis. Overload of tubular cells with filtered proteins has been shown to induce OPN expression in the proximal tubular epithelium in rat remnant kidney model in vivo, suggesting that proteinuria may be a strong inducer of tubular OPN expression [44]. However, the correlation of proteinuria with OPN expression in human renal diseases is rather conflicting [16, 45]. We could not find significant correlation between OPN expression and renal function or urinary protein excretion. This discrepancy between the clinical and pathogenic significance of OPN expression may be resulted from the antirejection treatment, the biopsy timing, or because of the diverse biologic functions of OPN. The diversity of its function may limit the prospect of being a promising target for immunosuppressive therapy.

In the present study, we demonstrated the up-regulated tubular expression of OPN at both the protein and mRNA levels in biopsies from renal allograft with acute rejection. OPN expression was correlated with interstitial macrophage infiltration and cell proliferation in both the tubular and interstitial compartments, supporting the role of OPN in macrophage recruitment and the subsequent proliferation and regeneration of tubulointerstitial cells in acute rejection.

ACKNOWLEDGMENTS

This work was supported in part by a Health and Labor Science Research Grants for Research on Specific Diseases from the Ministry of Health, Labor and Welfare (14164701, to F. Gejyo) and by a Grant-in-Aid for Scientific Research from the Ministry of Education, Culture, Sports, Science and Technology of Japan (16390242, to I. Narita). A part of this work has been presented at the 18th Niigata Symposium of Nephrology (Niigata, Japan, 2003). We thank Dr. Kota Takahashi and Dr. Kazuhide Saito from the Department of Urology, Niigata University for their kind support.

Reprint requests to Bassam Alchi, M.D., Division of Clinical Nephrology and Rheumatology, Niigata University Graduate School of Medicine and Dental Sciences, 1–757 Asahimachi-dori, Niigata 951–8510, Japan. E-mail: bassamalchi@hotmail.com

REFERENCES

1. Denhardt DT, Guo X: Osteopontin: A protein with diverse functions. *FASEB J* 7:1475–1482, 1993
2. Liaw L, Almeida M, Hart CE, *et al*: Osteopontin promotes vascular cell adhesion and spreading and is chemotactic for smooth muscle cells in vitro. *Circ Res* 74:214–224, 1994
3. Scatena M, Almeida M, Chaisson ML, *et al*: NF-kappaB mediates alphavbeta3 integrin-induced endothelial cell survival. *J Cell Biol* 141:1083–1093, 1998